universität wien

MASTERARBEIT / MASTER'S THESIS

Titel der Masterarbeit / Title of the Master's Thesis

„Spatio-Temporal Profiling of Filamin B mRNA in the mouse“

verfasst von / submitted by

Philipp Czermak BSc

angestrebter akademischer Grad / in partial fulfilment of the requirements for the degree of

Master of Science (MSc)

Wien 2018 / Vienna 2018

Studienkennzahl lt. Studienblatt / degree programme code as it appears on the student record sheet:	A 066 834
Studienrichtung lt. Studienblatt / degree programme as it appears on the student record sheet:	Masterstudium Molekulare Biologie
Mitbetreut von / Supervisor:	Univ.-Prof. Dr. Franz-Michael Jantsch

Index

Acknowledgements

I would like to thank Univ.-Prof. Dr. Michael Jantsch for giving me the chance to work on this exciting project, his constant support and inspiring discussions. A special thank goes to Ph.D. Laura Cimatti for her encouraging supervision, her trust in me to work independently, for all the assistance during the projects we were working on and for her patience that made it possible to publish this project. Especially, I would like to thank Aleksej Drino M.Sc. from the Mathias Schäfer group and Utkarsh Kapoor M.Sc. for their constant help, encouragement and scientific support whenever it was needed. I would also like to thank the other members of the Jantsch group and the members of the Center for Anatomy and Cell Biology for their support. Thanks to the Austrian Science Fund (FWF) for making this work possible.

Abbreviations

3’-UTR=	3 prime end untranslated region
ADAR=	Adenosine deaminase acting on RNA
ADAR1-c=	ADAR1p110 isoform
ADAR1-i=	ADAR1p150 isoform
ALS=	Amyotrophic lateral sclerosis
Alu-elements=	Arthrobacter luteus elements
AMPA=	α-amino-3-hydroxy-5-methyl-4-isoxazolepropionic acid
A-to-I=	Adenosine-to-Inosine
Bp=	Base pair
C451 and C516=	Cysteines at positions 451 and 516
cDNA=	Complementary deoxyribonucleic acid
chr=	Chromosome
CREB=	Cyclic adenosine monophosphate response element-binding protein
DNase I=	Deoxyribonuclease 1
DSH=	Dyschromatosis symmetrica hereditaria
dsRBD=	Double-stranded RNA-binding domain
dsRNA=	Double-stranded RNA
DSS1=	SEM1, 26S proteasome complex subunit
E12.5=	Embryonic stage 12.5
E396=	Glutamic acid at position 396
ECS=	Editing complementary sequence
EIE=	Editing inducer element
ES=	Editing site
ESCC=	Oesophagal squamous cell cancer
FLNA=	Filamin A

FLNB$^{-/-}$=	Filamin B homozygote knock-out
FLNB=	Filamin B
Gabra-3=	Gamma-Aminobutyric Acid Type A Receptor Alpha3 Subunit
GAPDH=	3-phosphate dehydrogenase
GLI1=	Glioma-associated oncogene
GluR=	Glutamate receptor
Gria2=	Glutamate Subunit 2
H394=	Histidine at position 394
hADAR1=	Human ADAR1
HCC=	Hepatocellular carcinoma
hnRNPs=	Heterogeneous nuclear ribonucleoproteins
HTR2C=	5-Hydroxytryptamine Receptor 2C
iSINE=	Inverted SINE
JNK1=	c-Jun N-terminal kinase 1
KPNA1 and KPNA3=	Karyopherin subunit α1 and α3
M/V=	Methionine/Valine
M2=	Melanoma 2 cell line
MAVS=	Mitochondrial antiviral-signalling protein
MDA5=	Melanoma differentiation-associated protein 5
miRNA=	Micro RNA
mRNA=	Messenger RNA
NEIL1=	Nei Like DNA Glycosylase 1
NES=	Nuclear export signal
NGS=	Next Generation Sequencing
NLS=	Nuclear localisation signal
NSCLC=	Non-squamous cell lung carcinoma

P=	Postnatal
PCR=	Polymerase chain reaction
PKR=	Protein kinase-R
pre-miRNA=	Precursor micro RNA
Q/R=	Glutamate/Arginine
RanGTP=	Ras-related nuclear protein guanosine triphosphate
RHOQ=	Ras homolog family member Q
RIG-I=	Retinoic acid-inducible gene I
RISC=	RNA-induced silencing complex
RNA=	Ribonucleic acid
RNAi=	RNA interference
RT-PCR=	Polymerase chain reaction on reverse transcribed cDNA
S/V=	Serine/Valine
SINE and LINE=	Short and long nuclear-interspersed element
STAU1=	Staufen homolog 1
TREX-2=	Transcription-Export 2
TRN1=	Transportin 1
VAI=	Virus-associated RNA I
VBCF=	Vienna Biocenter Core Facilities
wt=	Wild-type
WWP2=	WW domain-containing protein 2
XPO1=	Exportin 1
Zα and Zβ domain=	Z-DNA binding domains α and β

Abstract

RNA editing is a post-transcriptional modification which leads to nucleotide modifications, substitutions and insertion/deletion in RNA molecules. Adenosine-to-Inosine (A-to-I) editing is the main form of RNA editing in mammals and occurs in regions of double-stranded RNA (dsRNA). Adenosine deaminases acting on RNA (ADARs) are the RNA-editing enzymes involved in the deamination of adenosine to inosine. Filamin A (*FLNA*) messenger RNA (mRNA) is a highly conserved target of ADARs. In this study, we are especially interested in Filamin B (*FLNB*) mRNA editing levels in mouse. By amplicon sequencing, we were able to profile the editing levels of *FLNB* mRNA in various tissues during mouse development. We were able to detect high editing rates in blood, heart, muscle, fat and bones where the *FLNB* knockout mouse shows severe defects.

Introduction

Adenosine deaminases acting on RNA (ADARs)

ADARs are proteins which bind and harbour the capability to modify RNA. An adenine can get deaminated by hydrolysis whereby its amino group at C6 is exchanged with an oxygen atom. This process is called A-to-I editing and is facilitated by ADARs. The oxygen on C6 of inosine then can act as an acceptor to form a hydrogen bond. Due to this change of the interacting surface, the resulting inosine gets to be recognised as guanosine and the double-stranded structure may be stabilised since the majority of A-to-I editing events occur opposite of a cytosine (Wong et al. 2001).

Editing by ADARs through binding and deaminating double-stranded RNA post-transcriptionally is a conserved mechanism in metazoans (Nishikura et al. 2010). There are three ADAR enzymes expressed in humans (Figure 1). ADAR1 and ADAR2 are found in many tissues of the body, while the catalytically inactive ADAR3 is expressed only in the brain (Patterson and Samuel 1995). ADAR1 has two splice variants which differ in length: the shorter transcript encoding ADAR1p110 (ADAR1-c) is constitutively expressed, whereas the longer transcript ADAR1p150 (ADAR1-i) is interferon-inducible (George and Samuel 1999). Both versions of ADAR1 harbour a nuclear localisation signal (NLS). The long ADAR1p150 splicing variant contains an extranuclear export signal. Thus, ADAR1-c is mainly localised in the nucleus whereas the majority of ADAR1-i is localised in the cytosol. Also, both versions of the human ADAR1 protein exhibit an additional way of export which is dsRBD (double-stranded RNA-binding domain) and RNA-binding dependent (Fritz et al. 2009). In contrast, ADAR2 resides exclusively in the nucleus.

The common structural features of the ADAR family members are one or two dsRBDs and a deaminase domain at the carboxyterminal end of the proteins. The dsRBDs fold into a conserved α-β-β-β-α structure which facilitates direct contact to RNA. The longer ADAR1 isoform contains two Z-DNA binding domains (Zα and Zβ) on its N-terminus compared to one

Zβ domain in ADAR1-c. In contrast to its catalytically active family members, ADAR3 harbours an arginine-rich single-stranded RNA binding domain on the amino-terminal end and lacks Z-DNA binding domains (Chen et al. 2000).

The probable mechanism how ADARs facilitate the hydrolytic deamination of adenosines was uncovered by solving the crystal structure of ADAR2. A glutamic acid (E396) in the active site hydrogen bonds to water while two cysteines (C451 and C516) and a histidine (H394) residue coordinate a zinc ion. This zinc ion can activate the water molecule required for the nucleophilic hydrolytic deamination at C6 of adenines (Macbeth et al. 2005).

That said, ADAR1 or ADAR2 enzymes are capable of homodimerization in a dsRNA binding-independent manner (Valente and Nishikura 2007). In contrast, ADAR3 does not form dimers which could explain its inability to edit adenosine (Cho et al. 2003). Also, a study from 2006 shows that ADAR1 and ADAR2 form heterodimers (Chilibeck et al. 2006).

As mentioned, the two isoforms of ADAR1 are transcribed from separate promoters, one is constitutively expressed, and the other is interferon-inducible (George and Samuel 1999). In the brain, transcription activation of ADAR2 is regulated by CREB (cyclic adenosine monophosphate response element-binding protein) (Peng et al. 2006). In pancreatic β-cells, ADAR2 is regulated by JNK1 (c-Jun N-terminal kinase 1) (Yang et al. 2012). The localisation/shuttling of ADAR1 between the cytoplasm and nucleus differs depending on their localisation signal and interaction with importins and exportins as well as other interactors. As briefly described above ADAR1-i is exported from the nucleus by XPO1 (exportin 1) that recognises the nuclear export signal and is released in the cytoplasm by RanGTP (Ras-related nuclear protein guanosine triphosphate). Similarly, ADAR1-c can be exported despite lacking a nuclear export signal (NES). The export of the shorter isoform is facilitated by XPO5-RanGTP which is depended on dsRNA binding by the dsRBDs of ADAR1-c. Since both ADAR1 isoforms harbour an NLS, they both get imported by binding of Transportin 1 (TRN1) to the third dsRBD (containing the NSL). Binding of dsRNA can inhibit this mechanism. In contrast, ADAR2 is exclusively located in the nucleus since post-transcriptional modifications of the protein increases its stability and nuclear localisation positively. Unstable and unmodified ADAR2 that may reach the cytoplasm is targeted by E3 ubiquitin ligase WWP2 (WW domain-containing protein 2) and is rapidly degraded. Karyopherin subunit α1 (KPNA1) and KPNA3 are binding the N-terminal NLS of stable ADAR2 and are responsible for nuclear localisation of ADAR2 (Maas and Gommans 2009).

A general trend of mRNA editing during development can be detected and seems to be independent of the level of ADAR expression. The increase of A-to-I editing during development is mainly detected in the brain but not in non-brain tissue (Hwang et al. 2016; Tan et al. 2017). As we show in this study, a similar trend can be seen in brain tissue as well as most of the other tissues.

As mentioned, expression levels of ADARs do not necessarily correlate with the editing level of mRNAs. It was hypothesised that the pre-mRNA sequence and the structure near the

editing site (ES) contribute to target efficiency and specificity in pre-mRNA editing. Target specificity and to which extend the neighbouring nucleotides, the sequence or structural elements contribute to ADAR's A-to-I editing is poorly understood. It has been shown that ADARs prefer a distinct sequence and structure near the editing site that shows an imperfect helical structure (Eggington et al. 2011). This study also showed that preferred 5' neighbouring nucleotides for human ADAR1 (hADAR1) and hADAR2 are the same (U > A > C > G). Human ADARs show a slight difference in 3' preference for adjacent nucleotides: G > C ≈ A > U and G > C > U ≈ A for hADAR1 and hADAR2, respectively. They also confirmed the fact that ADARs can edit highly base-paired regions and adenines at the border of a stem that is preferentially not base-paired. This specificity seems to originate from ADARs catalytic domains since the exchange of the catalytic domains between hADAR1 and hADAR2 revealed that editing follows the identity of the catalytic domain rather than depending on the dsRBD. The mismatch of A:C in a double-stranded RNA structure shows higher editing when compared to mismatches like A:A, A:G or correct A:U base-pairing (Wong et al. 2001).

Concerning the structure, it has been shown that a stem at a distance from the editing site increases the efficiency and specificity of editing. This finding has been shown in the highly edited target of Gabra-3 (Gamma-Aminobutyric Acid Type A Receptor Alpha3 Subunit) (Daniel et al. 2017). This discovery led to the hypothesis of a general mechanism and the description of editing inducer elements (EIE). EIEs are characterised by a long stem that is separated from the editing site by a long internal loop. These structures seem to be able to induce editing independent of their sequence and localisation (up- or downstream) to the edited adenosine. Also, data implies that the large loop restricts the accessibility to the editing site adjacent to this loop that lies next to the EIE. The long stem of EIEs could act as a recruitment platform for dsRBD to bind and define the editing sites in addition to the C-terminal catalytic domain that specifically binds to the editing site by recognising its 5' and 3' preferred neighbouring nucleotides.

In general, inter- and intramolecular formed dsRNA elements bigger than twenty base pairs (bp) can be edited by ADAR (Nishikura et al. 1991). However, short dsRNA (about 20-30bp) and imperfect formed dsRNA with bulges and loops seem to be edited more selectively (Lehmann and Bass 1999), which accords with the discovery of EIEs as mentioned above. On the other hand, dsRNAs longer than hundred base pairs are hyper-edited. These regions are called hypermutations since about 50% of adenosines are edited in this region. These events can be observed for example during measle virus infection when viral ssRNA form large dsRNAs (Cattaneo et al. 1988).

A high throughput screen for potential proteins that might influence editing revealed that different proteins could modulate editing by direct or indirect interaction with ADARs or by directly interacting with mRNA, mRNA transport or by involvement in the splicing machinery, summarising these proteins being involved in the RNA metabolism. It has been shown that the increase of the SEM1, 26S proteasome complex subunit (DSS1) protein expression has a slight but significant positive effect on RNA editing (Garncarz et al. 2013). Amongst being part

of the S26 proteasome, DSS1 influences mRNA export, splicing and 3' end processing by interacting with heterogeneous nuclear ribonucleoproteins (hnRNPs) like the hnRNP proteins A2/B1 or the Transcription-Export 2 (TREX-2) complex. Hence, binding to hnRNPs may influence the mRNA transport, its metabolism or the processing of pre-mRNA. This regulatory mechanism of DSS1 on hnRNPs might lead to stabilisation of nascent pre-mRNA or influences folding that promotes recognition by ADARs and therefore increase editing. That said, dsRNA binding proteins may compete with ADAR, influencing its activity by competition or by antagonization. One antagonising enzyme lies within the ADAR family itself. ADAR3 can act as an ADAR2 inhibitor by competing with its RNA substrate (Chen et al. 2000). In contrast to ADAR2, whose regulation in the nucleus by antagonising enzymes is unknown, ADAR1 and its adversaries are better studied. Viral RNAs and proteins can impair ADAR1s activity (George et al. 2009). Adenovirus VAI RNA that is a small highly structured RNA and is required in late infection can inhibit ADARs editing activity (Lei et al. 1998). It is also speculated that both, RNA binding by ADARs and RNA interference (RNAi), are competing mechanisms (Wu et al. 2011). Whether other dsRBD containing proteins like protein kinase-R (PKR) or STAU1 (Double-stranded RNA-binding protein Staufen homolog 1) that bind mRNA act antagonistic, competing or other potential regulators of ADARs exist must be examined in more detail.

Developmentally, *ADAR1* is an important and essential gene in humans and mice, and it has been shown that ADAR-like enzymes are active in all metazoan tissues (Hung et al. 2017) ADAR1 is ubiquitously expressed in mice. ADAR1 knockout mice die at embryonic stage 12.5 (E12.5) supporting the importance of ADARs. That said, ADARs play a crucial role in recognising endogenous versus exogenous RNA sources. Editing is indicated to mark "self" RNA so that "non-self" RNAs like the ones originating from viruses are recognised as foreign RNA sources. Interferon induction may be induced through recognition of non-edited RNA. Further, unedited RNA can be recognised by melanoma differentiation-associated protein 5 (MDA5) and Retinoic acid-inducible gene I (RIG-I) which further activates mitochondrial antiviral-signalling protein (MAVS) (Mannion et al. 2014). However, also foreign RNA can be edited to inhibit its RNA function as it has been shown in Epstein-Barr virus (Lei et al. 2013). These findings indicate that the phenotype of ADAR1 knockout mice may derive from constant interferon response, but more ADAR targets and the exact cause of death at this early stage remains to be investigated. Other characteristics of ADAR1 knockout mice besides elevated activation of interferon signalling are aberrant apoptosis (Wang et al. 2004) and erythropoiesis in the liver (Hartner et al. 2009; XuFeng et al. 2009) which are also very likely to contribute to this embryonic lethality.

ADAR2 is found in many tissues but is mainly expressed in the nervous tissue where it plays an essential role in function as described below. Whereas, ADAR3 whose deaminating function still has to be shown, is exclusively expressed in the brain. In the brain, the main ADAR2 pre-mRNA targets are G-protein coupled receptors, ligand-gated and voltage-gated channels. $ADAR2^{-/-}$ mice undergo severe seizures and epilepsy within three weeks of age. It has been proven that this phenotype is displayed due to lack of editing in Glutamate Subunit 2 (Gria2)

pre-mRNA since the respective protein can rescue the phenotype (Higuchi et al. 1993 and 2000).

Various diseases in humans arise from mutations in the ADAR genes. Illnesses deriving from aberrant editing are best studied in brain tissues and well characterised in humans. Since editing of the glutamate receptor (GluR) by ADAR2 is necessary to regulate the Ca^{2+} permeability of the α-amino-3-hydroxy-5-methyl-4-isoxazolepropionic acid (AMPA) receptor, lost or reduced editing events in this mRNA results in increased Ca^{2+} influx. Under-editing by ADAR2 has been reported in brain tumours like the glioblastoma multiform, lung, kidney and testis (Maas et al. 2001; Paz et al. 2007). Sporadic amyotrophic lateral sclerosis (ALS) is also associated with a drastic decrease in the editing of GluR. Editing of the 5-HT_{2C} serotonin receptor pre-mRNA by ADARs results in up to 24 isoforms of this enzyme (Burns et al. 1997). Aberrant editing may lead to neurological disorders like depression and suicide (Bhansali et al. 2007; Gurevich et al. 2002). Several ADAR1 mutations can cause the development of a skin disorder called dyschromatosis symmetrica hereditaria (DSH) and the occurrence of other neurological defects like dystonia and mental deterioration (Miyamura et al. 2003; Tojo et al. 2006). These findings demonstrate the importance of ADARs in the brain and other organs to edit specific protein-coding mRNAs.

Diseases with aberrant editing in coding transcripts by ADARs are indicated to have an influence on cancer formation, either by hypo- or hyper-editing. Increased editing of Nei Like DNA Glycosylase 1 (NEIL1) by ADAR1-i was identified in non-squamous cell lung carcinoma (NSCLC) (Yeo et al. 2010). The chloride channel GABRA3 edited by ADAR1-c is shown to be hypo-edited in breast cancer (Gumireddy et al. 2016). The Ras homolog family member Q (RHOQ) undergoes an Asparagine to Serine substitution. Elevated editing of RHOQ increases invasiveness of tumour cells and is associated with colorectal cancer, gastric cancer and NSCLC (Han et al. 2014). The glioma-associated oncogene (GLI1) is a transcription factor in the hedgehog signalling pathway and is a substrate of both ADAR1 and ADAR2. Editing of this factor appears to reduce its oncogenic potential and is found to be hypo-edited in tumour cells (Shimokawa et al. 2013). Whether ADAR1 or ADAR2 edit the hematopoietic cell tyrosine phosphatase (PTP6) is unclear, but it is known that higher editing is linked to acute myeloid leukaemia (AML) (Beghini et al. 2000). Hyper-editing of AZIN1 mRNA by ADAR1 is linked to oesophagal squamous cell cancer (ESCC) and hepatocellular carcinoma (HCC) (Chan et al. 2014; Qin et al. 2014). As well as AZIN1, *FLNB* mRNA is found to be hyper-edited in ESCC, but its precise involvement in cancer development is unknown.

A-to-I editing has a great impact on gene expression. In fact, Inosine is recognised as guanine by cellular machineries responsible for splicing, translation, folding and miRNA silencing. Thus, the effect of an A-to-I editing event is manifold and depends on its localisation along the RNA transcript. Even though A-to-I editing seems to play an important role in development, it mainly takes place in non-coding regions like short and long nuclear-interspersed elements (SINEs and LINEs) (Ramaswami et al. 2013). In humans, the most abundant SINE-like retrotransposons are Alu-elements. They can be edited when repeats are inverted and form

double-stranded RNA structures. Mice lack Alu-elements but harbour B1 and B2 repetitive elements as SINE representatives (Danecek et al. 2012). These elements can insert into intronic regions, untranslated regions (UTRs) or exons of coding genes and can, therefore, influence gene expression by, for example, altering splicing patterns when inserted in introns (Lev-Maor et al. 2008). Also, it has been proposed that editing of inverted SINEs (iSINEs) may play a role in down-regulating gene expression. It has been shown that editing of iSINEs in 3'-UTRs (3 prime end untranslated regions) is not only structural but also sequence-dependent and that translational retention of these products is independent of dsRNA binding proteins like ADARs (Tajaddod et al. 2016).

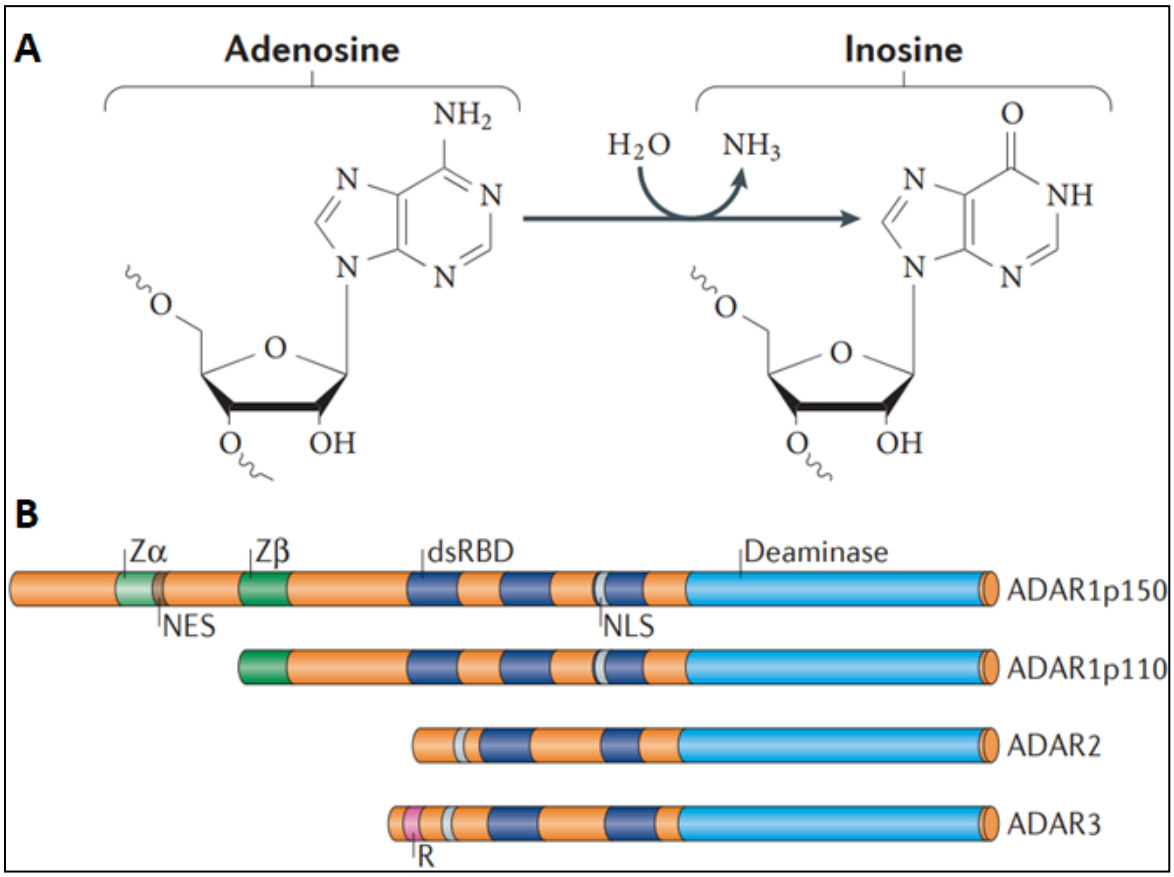

Figure 1: Adenosine deamination by ADAR proteins. (A) Hydrolytic deamination facilitated by ADARs eliminates the amine on the C6 atom of adenine and introduces oxygen. (B) Scheme of the three human ADAR family members. Both ADAR1 isoforms harbour Z-DNA binding domains, shown in dark and light green. All ADAR proteins contain two to three dsRNA binding domains depicted in dark blue and a catalytic deaminase domain (light blue). The R domain (purple) along the ADAR3 protein binds single-stranded RNAs. The nuclear export signal directly follows the Z-DNAα binding domain in the ADAR1-i isoform, whereas the nuclear localisation signal is localised in the third dsRBD and is present in both ADAR1 isoforms (Nishikura 2015).

Concerning splicing, an editing event may lead to elimination and/or creation of a splice site (Rueter et al. 1999; Farajollahi et al. 2010). When a 3'-AG splicing acceptor site is edited, splicing is impaired. Conversely, if an AA-site is edited in the second adenosine, it can be recognised as a new acceptor site. Cryptic splice sites may result in different protein variants

(Dillman et al. 2016). For example, by editing its own transcript, ADAR2 introduces an alternative splicing acceptor site that gives origin to a truncated version of ADAR2 lacking the dsRNA binding domain. Therefore, this truncated ADAR2 functions as a negative feedback regulatory mechanism. Interestingly, when an A-to-I editing event is localised in the coding region of a mRNA, recoding during translation may lead to non-synonymous amino acid substitutions or premature truncation of the encoded protein.

If a protein-coding mRNA is edited and depending on the position of edited adenosine, the protein function and stability may change positively or negatively (Stellos et al. 2016). *Gria2* mRNA editing is an example of non-synonymous substitution. *Gria2* codes for a subunit GluA2 of the glutamate receptor whose Q/R site is found to be almost constantly edited (Sommer et al. 1991). Gria2 has two editing sites that have different effects when edited. One editing site (R/G site) leads to faster recovery from desensitisation when edited (Lomeli et al. 1994; Krampfl et al. 2002). Hyper-editing of this site in GRIA2 mRNA leads to seizures in mice. In the second site (Q/R site) of this AMPA sensitive glutamate receptor, editing decreases Ca^{2+} permeability. Therefore, lack of editing at this site increases the risk of seizures and a high risk of death within the first weeks of age in mice (Brusa et al. 1995). ADAR2 knockout mice ($ADAR2^{-/-}$) that lack Gria2 editing can be rescued by introducing fully edited Gria2 ($GluA^{R/R}$) (Higuchi et al. 2000). Similarly, *Gabra3* gets edited in the brain which likewise modulates its permeability to chloride. Also, the G protein couples serotonin receptor 5-HT_{2C}R (Burns et al. 1997) and the potassium channel Kv1.1 (Bhalla et al. 2004) are edited in an ADAR-depended manner. This event is believed to contribute to development since editing starts post-natal and increases in newborn mice from 50% to almost 100% in adult mice.

ADAR2 has been shown to bind to pre-miRNA (precursor micro RNA) and regulate their maturation and expression, which increases the diversity or the miRNome (Vesely et al. 2012). MiRNA target specificity may change due to A-to-I editing affecting pathway regulation or target populations. In humans, the disruption of miRNA/mRNA binding sites may result in neurodegenerative, cardiovascular, and carcinogenic diseases (Nigita et al. 2015). It has been shown that ADAR1 may bind to Dicer and upregulate its activity to process pri-miRNAs. An increase in mRNA silencing has been shown by binding of ADAR1 to miRNA and loading it to RISC (RNA-induced silencing complex) (Ota et al. 2013). On the contrary, the opposite effect has been reported, when editing of pre-miRNAs by ADAR1 has a negative effect on miRNA processing and maturation (Kawahara et al. 2007). Editing of miRNAs has also been shown to play an important role in Epstein-Barr viral infection by editing the virus RNA and therefore suppressing RISC loading (Iizasa et al. 2010).

A-to-I editing of RNA serves as a dynamic remodelling system of the transcriptome, providing another level of complexity with high mRNA variability and proteome diversity.

Filamins

Three isoforms of filamins are known in vertebrates. Filamin A (*FLNA*) and Filamin B (*FLNB*) are ubiquitously expressed actin-crosslinking proteins (Sheen et al. 2002) whereas Filamin C (*FLNC*) is expressed in skeletal and heart muscle (Chakarova et al. 2000). Filamin proteins consist of 24 immunoglobulin-like repeats, which are separated by two hinge regions into two-rod domains and a self-association domain (Stossel et al. 2001; Pudas et al. 2005). Filamins can form homo- or heterodimers which crosslinks actin filaments and bind them to the cell membrane to support cell shape, locomotion and morphology (Popowicz et al. 2006, Nakamura et al. 2011). Different alternative splice variants of filamin have been shown to exhibit different cross-linking activity (Brotschi et al. 1978). Shear stress may disrupt filamin-actin networks, and binding activity seems to be dependent on the filamin to F-actin ratio (Janmey et al. 1990; Gorlin et al. 1990). The amino terminus of filamins provides the actin-binding site to form a three-dimensional filament network, whereas the carboxy-terminal end of filamins binds several transmembrane receptors, ion channels and signalling molecules (Stossel et al. 2001; Zhou et al. 2010) (Figure 2). Deletion or mutation in filamins results in drastic changes in cellular processes and diseases.

Filamins provide different biological functions and are highly conserved in their genomic organisation. Between the exon-intron structure and the repeated protein domains no correlation can be drawn (Patrosso et al. 1994; Chakarova et al. 2000). Multiple orthologs have been identified in other species like Drosophila (filamin-240) that are shorter compared to vertebrate's filamins. The expression is regulated through alternative promotors, as shown in chicken (Barry et al. 1993), and alternative isoforms of filamins may also arise due to alternative splicing of pre-mRNA, as shown for the short version of *FLNA* (Gorlin et al. 1990). Interestingly, isotype switching during development may display an interesting involvement of filamins in myogenesis (Gomer et al. 1983). Tissue-specific expression, in particular for *FLNC*, may contribute to a specific function in certain organs (Thompson et al. 2000). However, most studies do not discriminate between the different filamin isoforms. Thus, the functional role of each filamin variant needs further investigations.

As mentioned, filamins exhibit a highly interacting C-terminal domain that binds different enzymes involved in cellular processes. The glycoprotein-Ibα (GP-Ibα) is a well-studied interaction partner of *FLNA* and *FLNB*. GP-Ibα is a subunit of the heteropentameric GPIb-factor (vWF) receptor, and its interaction with filamins upon activation regulates cytoskeletal rearrangements and platelet activation (Takafuta et al. 1998; Fox et al. 1985). Additionally, FLNA splice variants are shown to bind the cytoplasmic domain of different integrins with a different affinity (Pfaff et al. 1998; Meyer et al. 1998; van der Flier et al. 2002). Filamins bind several other membrane proteins, receptors and signalling proteins. Several GTPases can bind to filamins (Ueda et al. 1992; Ohta et al. 1999; Bellanger et al. 2000) and kinases acting on filamins influence this interaction. Moreover, filamins are susceptible to proteolysis and

binding of other proteins like GTPases is very likely to be phosphorylation-dependent (Yada et al. 1990; Jay et al. 2000; Leonardi et al. 2000). The exciting interplay between filamins and their interacting partners must be further investigated for a better understanding of the involvement of filamins in various cellular pathways.

At the organismal level, it has been shown that Flnb is an essential gene which plays a key role in bone development. In mice, loss of *FLNB* gene results in lethal skeletal disorders, such as short stature and spondylocarpotarsal synostosis syndrome, progressive vertebral fusion, disc degeneration and ossification of cartilage due to upregulation of TGF-ß and BMP signalling (Zieba et al. 2016).

Loss-of-function mutations or deletion of the *Flna* gene (chrX: 74,223,461-74,249,820; GRCm38.p6) are embryonically lethal in mice. Their phenotype may also be associated with skeletal dysplasia, but lethality is mainly due to cardiovascular defects and disrupted neuronal migration (Zhou et al. 2007; Hart et al. 2006; Feng et al. 2006). These defects mirror the human syndromes caused by mutations in FLNA and FLNB (Online Mendelian Inheritance in Man, OMIM®. Johns Hopkins University, Baltimore, MD. MIM Number: *300017 and *603381, respectively). In humans, *FLNA* is located at chrX: 154,348,526-154,374,638 (GRCh38.p12). In mouse and human, the pre-mRNA transcript of *FLNA* is edited in exon 42, and they consist of 47 and 48 exons, respectively. The highly homologous *FLNB* transcript is edited in the very same exonic position. Comparison of exon-intron structure between *FLNA* and *FLNB* pre-mRNAs shows a sequence for intron 42 which is longer in *FLNB* than in *FLNA*. This longer sequence results in an editing complementary sequence (ECS) which lies closer to the editing site in *FLNA* pre-mRNA than in *FLNB* pre-mRNA. ECSs are complementary sequences to the editing site that are mandatory for dsRNA formation and editing of RNA by ADARs since it binds and forms internal double-stranded structures by complementarity.

In mice the *Flnb* gene is encoded on chromosome 14 (GRCm38.p6: 7,817,957-7,951,588), while in human Flnb is encoded on chromosome 3 (GRCh38.p12 58,008,400-58,172,251). In mice as well as in humans, the *Flnb* transcript consists of 46 exons. The transcript of the *Flnb* gene results in a pre-mRNA of 133.631 nucleotides and a protein that is 2602 amino acids in length.

Both *FLNA* and *FLNB* mRNA are known conserved coding targets of A-to-I editing by ADARs. In humans and mice *FLNA* (chrX: 74,226,860 in mouse; chrX: 154,351,580 in human) and *FLNB* (chr14: 7,936,048 in mouse; chr3: 58,159,685 in human) undergo A-to-I editing at the same position in exon 42 and in mice results in a Q/R exchange in the amino acid 2296 or 2333 of repeat 22 in the FLNB and FLNA protein, respectively (Li et al. 2009). Additionally, in the Flnb transcript, a second editing site upstream of the Q/R site has been discovered (Bahn et al. 2011). In humans, editing at this position (chr3: 58,159,678) results in an exchange from Methionine to Valine (M/V) in humans. In mice, the secondary editing event is located in the downstream triplet (chr14: 7,936,041) and results in a Serine to Valine (S/V) exchange. The

region affected is a very interactive domain and amino acid substitutions likely result in altered binding specificities for interacting proteins.

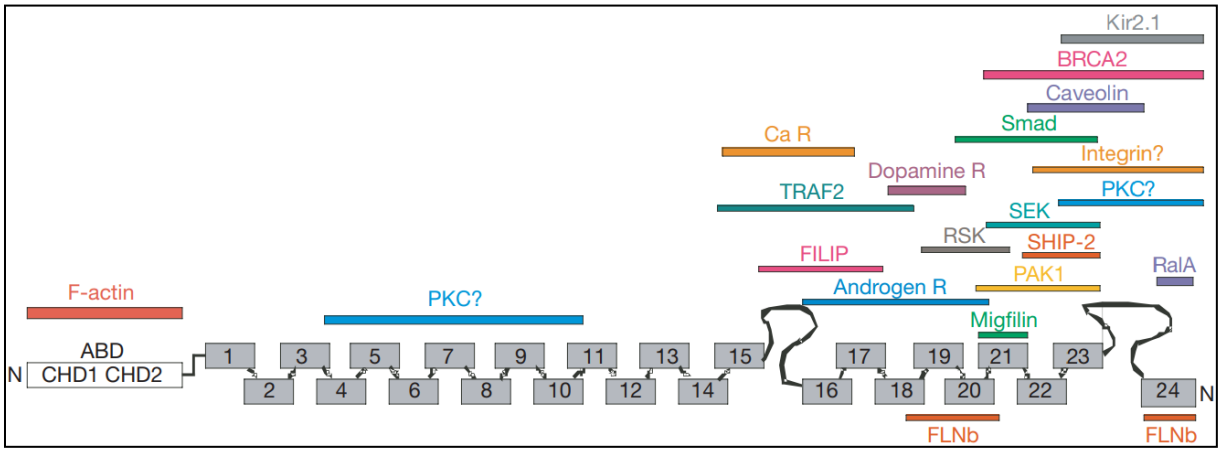

Figure 2: Schematic structure of filamins and their protein interactors. N-terminal actin-binding domain (ABD) contains two calponin homology domains (CHD1 and CHD2). Two hinge domains divide the following 24 Ig-like repeats and mediate interaction with more than 90 proteins. The C-terminal repeat 24 facilitates filamin homo- or heterodimerization (Feng and Walsh 2004).

Aim

Until recently editing of coding substrates was believed to occur primarily in the brain. The major focus for the last two decades lies within the identification of ADAR's role in this organ. However, there are about hundred protein-coding substrates known to date. Close analysis of some protein-coding targets indicates that editing can also be high outside the nervous system. For instance, editing of Filamin A pre-mRNA was found to be highest in the vascular tissue and the digestive tract where editing levels reach almost 100%. The importance of *FLNA* mRNA editing in cardiovascular and heart physiology (Jain et al. 2018) showed that the relevance of A-to-I editing in other coding transcripts might be as relevant as in the brain. Consequently, lack of editing will most likely manifest itself in certain phenotypes in those tissues where editing is highest.

To get a better understanding on the functional role of Filamin B editing and to facilitate future phenotypic analysis of mice altered in FLNB editing we aimed to decipher the Spatio-temporal distribution of FLNB editing during mouse development. This was achieved by performing amplicon sequencing of the respective editing site in Filamin B mRNA. Therefore, tissues from neonate (P0), juvenile (P21) and adult (P120) wild-type (wt) C57BL/6J mice were collected and RNA extraction performed. The extracted RNA was reverse transcribed, and the target of interest enriched by polymerase chain reaction (PCR). In details, the forward and reverse PCR primers were designed around the *Flnb* editing site (exon 42) on two consecutive exons (42 and 43). In the second round of PCR, a dual-indexed set of primers were used to differentiate tissue and developmental stage of each sample. The pool of barcoded amplicons where then sequenced on an Illumina platform and subsequently analysed for editing.

Materials and methods

Mice

Male wild-type (C57BL/6J) mice were sacrificed at birth (P0), 21 days and 120 days after birth (P21 and P120, respectively). Dissected organs were snap frozen in liquid nitrogen and either immediately used for total RNA extraction or stored at -80°C.

RNA extraction using the peq GOLD TriFast™ reagent

Tissues were homogenised in 1ml TriFast™ reagent with the help of scissors and pestle. The total volume of added TriFast™ reagent equals at least 90% of the tissue's weight. Scissors and pestle were cleaned after every sample by washing them sequentially in: ddH2O, 5% sodium hypochlorite, ddH2O, 1M NaOH, ddH2O and 70% EtOH. After homogenization, samples were mixed thoroughly and incubated at room temperature (rt) for 10 minutes. After the addition of 0.2 ml chloroform samples were vigorously mixed for approximately 15 seconds and kept at rt for 10 minutes before centrifugation at 12 000g for 10 minutes. The aqueous phase was transferred into a new RNase free tube, and 0.5ml isopropanol was added. Samples were precipitated at -20°C overnight (o/n). After centrifugation at 12 000g for 10 minutes, the supernatant was removed. The RNA pellets were then washed twice with 70% EtOH. The supernatant was removed, and pellets were air-dried at room temperature. Eventually, the pellets were resuspended in 50µl ddH_2O and heated at 55°C for 5 minutes. For downstream applications, UV absorption was used to quantify the extracted RNA.

RNA extraction using commercial kits

The "PerfectPure^{tm} RNA Cell & Tissue" kit from 5Prime or the "E.Z.N.A.® Tissue RNA Kit" from Omega Bio-Tek were used according to the company's instructions.

RNA agarose/formaldehyde gel and sample preparation

The instruments and working space under the laminar flow hood were cleaned with RNaseZap (Ambion®).

For the gel: 1 g of agarose powder was dissolved in 60ml ddH_2O. This solution was cooled down to approximately 60°C before adding 9ml of 10xMOPS (3-(N-morpholino)-propanesulfonic acid) and 16.5ml of 37% formaldehyde. After thoroughly mixing the solution was poured into the gel-chamber.

For one litre of 10xMOPS buffer: 41.2g of MOPS (powder), 4.1g of sodium acetate and 3.7g of EDTA were dissolved in ddH_2O, and the pH was adjusted to 7 by using NaOH (1M).

For the running buffer: 50ml of 37% formaldehyde and 50ml of 10xMOPS were mixed in a final volume of 500ml.

For the 3x RNA loading buffer: 500µl formamide, 100µl 10xMOPS, 167µl 37% formaldehyde, 100µl 100% glycerol, 5µl ethidium bromide [10 mg/ml] and 0.5% bromphenol blue were dissolved in DEPC H_2O to a final volume of 1ml.

Sample preparation: for every sample 1µg of RNA was diluted in ddH2O to a final volume of 6µl, then 3µl of 3x loading buffer were added, after 5 minutes at 65°C samples were chilled on ice and loaded onto the gel.

Running conditions: 90V for at least 30 minutes.

DNase I digestion

5µg of total RNA was digested with 5U of RNase free DNase I (Thermo Fisher Scientific) in the presence of 1.25U of Ribolock RNase inhibitor (Thermo Fisher Scientific) in 1x DNase buffer for a final volume of 50µl. Samples were incubated at 37°C for one hour. To inactivate the enzyme5µl of 50mM EDTA were added, and samples were incubated at 65°C for 10 minutes.

Reverse Transcription

0.5µg of DNase I digested RNA was reverse transcribed with the Revert Aid reverse transcriptase (Thermo Fisher Scientific) following the manufacturer's instructions. Briefly, random hexamers were added to the RNA, incubated at 65°C for 5 minutes and immediately chilled on ice to disrupt secondary structures. RT buffer, dNTPs and 1µl reverse transcriptase (RT^+) or ddH2O (RT^-) were added. After 10 minutes at room temperature, the samples were incubated at 42°C for one hour. To inactivate the reverse transcriptase, samples were heated at 70°C for 10 minutes.

Polymerase chain reaction

Reverse transcription check

For quality control of reverse transcribed mRNA, the following primers were used:

MJ 3467: forward primer 5'-CAGCCCTTACCTGGTGCCCGT-3'

MJ 3468: reverse primer 5'-CTTTGCATCAATCTTCCCTTTCG-3'

The PCR reaction for these controls always contained the following solutions:

2.5µl 10x Taq Buffer
2.5µl MgCl2 [25mM]
0.5µl dNTP Mix [10mM]
0.8µl of each primer [10µM]
0.5µl Taq DNA Polymerase
1.5µl cDNA
ddH2O to a final volume of 25µl

The PCR machine was programmed as follows:

1) 95°C for 5 minutes
2) 95°C for 1 minute
3) 60°C for 45 seconds
4) 72°C for 30 seconds
5) repeat from step 2) 34 times
6) 72°C for 10 minutes
7) 4°C

PCR samples were run on a 2% agarose gel and bands at the expected height were gel-extracted with Promega's "Wizard® SV Gel and PCR Clean-Up System" kit following the provided instructions. Each sample was eluted in 30µl ultra-pure water.

Generating amplicons containing Filamin B editing site flanked by adaptors

The following PCR was performed on reverse transcribed products that show no product in the RT check (see above):

MJ 5353: Forward primer 5'-ACACGACGCTCTTCCGATCTTCGCTGCCTCACTGTTCTGAG-3'

MJ 5354: Reverse primer 5'-CAGACGTGTGCTCTTCCGATCTCGCTGGCTGGTTAACTTTTAATC-3'

The PCR reactions for this approach always contained the following solutions:

5µl	Q5 Buffer
0.5µl	dNTP Mix [10mM]
1.25µl	of each primer [10µM]
0.25µl	Q5 Polymerase
1.5µl	cDNA (RT^+)
ddH2O	to a final volume of 25µl

The PCR machine was programmed as follows:

1) 98°C for 4 minutes
2) 98°C for 10 seconds
3) 55°C for 20 seconds
4) 72°C for 30 seconds
5) repeat from step 2) 24 times
6) 72°C for 5 minutes
7) 4°C

PCR samples were directly purified using silica matrices ("Wizard® SV Gel and PCR Clean-Up System" kit from Promega) following the provided instructions. Each sample was eluted in 30µl ultra-pure water.

Transformation with pGEM®-T Easy Vector System

To transform E. coli (DH5alpha) with pGEM®-T easy vector harbouring desired product, we followed Promega's provided protocol. Cells were seeded on LB/ampicillin/IPTG/X-Gal plates and grown at 37°C overnight. Five ml of LB/ampicillin media was inoculated with selected white colonies and grown overnight at 37°C shaking. Tubes with cultured cells were spun for 10 minutes at 3500 rpm. The supernatant was removed, the pellet was resuspended in 100µl P1 Buffer and incubated for 3 minutes at room temperature. Per colony, 200µl P2 Buffer was added, and tubes were inverted 4 to 6 times and left on ice for 3 minutes. Then 150µl P3 Buffer was added and again inverted 4 to 6 times and kept on ice for 3 minutes. These samples were then centrifuged at maximum speed for 10 minutes. The supernatant, 450µl per sample, was transferred into a new tube and 1 ml of cold 96% Ethanol was added and kept on -20°C for approximately 30 minutes. Samples were then spun at 14000 rpm for 10 minutes and washed with 70% Ethanol. After another spin, the pellets were air-dried under the hood and resuspended in 50µl ultra-pure water.

P1 Buffer: 50mM Tris/HCl pH 8, 10mM EDTA, RNAse A (0.1 mg/ml)

P2 Buffer: 1% SDS, 0.2 M NaOH

P3 Buffer: 3M KAc/HAc pH 5.5

PCR to generate indexed amplicons for NGS

The following PCR was performed on PCR products that contain the *Flnb* mRNA editing site (see above) and are flanked by adaptors (workflow see figure 3):

NEB NEXT index Primer i5: Forward primer

5'-AATGATACGGCGACCACCGAGATCTACAC**[i5]**ACACTCTTTCCCTACACGACGCTCTTCCGATCT-3'

NEB NEXT index Primer i7: Reverse primer

5'-CAAGCAGAAGACGGCATACGAGAT**[i7]**GTGACTGGAGTTCAGACGTGTGCTCTTCCGATCT-3'

Were i5 and i7 corresponds to the twenty different barcodes that each consist of 8 different bases (see table 1).

The PCR reactions for this approach always contained the following solutions:

5µl	Q5 Buffer
0.5µl	dNTP Mix [10mM]
1.25µl	of one i7 indexed primer
1,25µl	of one i7 indexed primer
0.25µl	Q5 Polymerase
10µl	PCR product with adaptors (see above)
ddH2O	to a final volume of 25µl

The PCR machine was programmed as follows:

1) 98°C for 4 minutes
2) 98°C for 10 seconds
3) 55°C for 20 seconds
4) 72°C for 30 seconds
5) repeat from step 2) 14 times
6) 72°C for 5 minutes
7) 4°C

PCR samples were run on a 2% agarose gel and bands at the expected height (194bp) were gel-extracted with Promega's "Wizard® SV Gel and PCR Clean-Up System" kit following the provided instructions. Each sample was eluted in 30µl ultra-pure water.

The DNA concentration of the eluted samples was quantified by fluorimetric assay (Invitrogen™ Qubit™ 3.0 Fluorometer, Thermo Fisher Scientific) and samples were pooled accordingly.

The overall process of cluster generation, sequencing, image processing, demultiplexing, and quality score calculation was performed at the VBCF NGS Unit (www.vbcf.ac.at).

Obtained reads were mapped against the full-length amplicon sequence using bwa mem40 with default settings, and base occurrence was deduced using bam-readcount (https://github.com/genome/bam-readcount) with the minimal base quality parameter and the minimal read mapping quality set to 20. All mouse genome coordinates mentioned refer to the genome assembly GRCm38/mm10.

Table 1: List of Primers used for PCR to generate barcoded amplicons for NGS. This list was provided in NEBs library preparation user manual (NEBNext® Multiplex Oligos for Illumina® (Dual Index Primers Set 1)).

NEB #	PRODUCT	INDEX PRIMER SEQUENCE	EXPECTED INDEX PRIMER SEQUENCE READ
#E7603A: 0.060 ml	NEBNext i501 Primer	5´-AATGATACGGCGACCACCGAGATC-TACACTATAGCCTACACTCTTTCCCTA-CACGACGCTCTTCCGATC*T-3´	TATAGCCT
#E7604A: 0.060 ml	NEBNext i502 Primer	5´-AATGATACGGCGACCACCGAGATC-TACACATAGAGGCACACTCTTTCCCTA-CACGACGCTCTTCCGATC*T-3´	ATAGAGGC
#E7605A: 0.060 ml	NEBNext i503 Primer	5´-AATGATACGGCGACCACCGAGATC-TACACCTATCCTACACTCTTTCCCTA-CACGACGCTCTTCCGATC*T-3´	CCTATCCT
#E7606A: 0.060 ml	NEBNext i504 Primer	5´-AATGATACGGCGACCACCGAGATC-TACACGGCTCTGAACACTCTTTCCCTA-CACGACGCTCTTCCGATC*T-3´	GGCTCTGA
#E7607A: 0.060 ml	NEBNext i505 Primer	5´-AATGATACGGCGACCACCGAGATC-TACACAGGCGAAGACACTCTTTCCCTA-CACGACGCTCTTCCGATC*T-3´	AGGCGAAG
#E7608A: 0.060 ml	NEBNext i506 Primer	5´-AATGATACGGCGACCACCGAGATC-TACACTAATCTTAACACTCTTTCCCTA-CACGACGCTCTTCCGATC*T-3´	TAATCTTA
#E7609A: 0.060 ml	NEBNext i507 Primer	5´-AATGATACGGCGACCACCGAGATC-TACACCAGGACGTACACTCTTTCCCTA-CACGACGCTCTTCCGATC*T-3´	CAGGACGT
#E7610A: 0.060 ml	NEBNext i508 Primer	5´-AATGATACGGCGACCACCGAGATC-TACACGTACTGACACACTCTTTCCCTA-CACGACGCTCTTCCGATC*T-3´	GTACTGAC

NEB #	PRODUCT	INDEX PRIMER SEQUENCE	EXPECTED INDEX PRIMER SEQUENCE READ
#E7611A: 0.040 ml	NEBNext i701 Primer	5´-CAAGCAGAAGACGGCATACGAGA-TCGAGTAATGTGACTGGAGTTCAGAC-GTGTGCTCTTCCGATC*T-3´	ATTACTCG
#E7612A: 0.040 ml	NEBNext i702 Primer	5´-CAAGCAGAAGACGGCATACGAGA-TTCTCCGGAGTGACTGGAGTTCAGAC-GTGTGCTCTTCCGATC*T-3´	TCCGGAGA
#E7613A: 0.040 ml	NEBNext i703 Primer	5´-CAAGCAGAAGACGGCATACGAGA-TAATGAGCGGTGACTGGAGTTCAGAC-GTGTGCTCTTCCGATC*T-3´	CGCTCATT
#E7614A: 0.040 ml	NEBNext i704 Primer	5´-CAAGCAGAAGACGGCATACGAGA-TGGAATCTCGTGACTGGAGTTCAGAC-GTGTGCTCTTCCGATC*T-3´	GAGATTCC
#E7615A: 0.040 ml	NEBNext i705 Primer	5´-CAAGCAGAAGACGGCATACGAGA-TTTCTGAATGTGACTGGAGTTCAGAC-GTGTGCTCTTCCGATC*T-3´	ATTCAGAA
#E7616A: 0.040 ml	NEBNext i706 Primer	5´-CAAGCAGAAGACGGCATACGAGA-TACGAATTCGTGACTGGAGTTCAGAC-GTGTGCTCTTCCGATC*T-3´	GAATTCGT
#E7617A: 0.040 ml	NEBNext i707 Primer	5´-CAAGCAGAAGACGGCATACGAGA-TAGCTTCAGGTGACTGGAGTTCAGAC-GTGTGCTCTTCCGATC*T-3´	CTGAAGCT
#E7618A: 0.040 ml	NEBNext i708 Primer	5´-CAAGCAGAAGACGGCATACGAGA-TGCGCATTAGTGACTGGAGTTCAGAC-GTGTGCTCTTCCGATC*T-3´	TAATGCGC
#E7619A: 0.040 ml	NEBNext i709 Primer	5´-CAAGCAGAAGACGGCATACGAGA-TCATAGCCGGTGACTGGAGTTCAGAC-GTGTGCTCTTCCGATC*T-3´	CGGCTATG
#E7620A: 0.040 ml	NEBNext i710 Primer	5´-CAAGCAGAAGACGGCATACGAGA-TTTCGCGGAGTGACTGGAGTTCAGAC-GTGTGCTCTTCCGATC*T-3´	TCCGCGAA
#E7621A: 0.040 ml	NEBNext i711 Primer	5´-CAAGCAGAAGACGGCATACGAGAT-GCGCGAGAGTGACTGGAGTTCAGAC-GTGTGCTCTTCCGATC*T-3´	TCTCGCGC
#E7622A: 0.040 ml	NEBNext i712 Primer	5´-CAAGCAGAAGACGGCATACGAGA-TCTATCGCTGTGACTGGAGTTCAGAC-GTGTGCTCTTCCGATC*T-3´	AGCGATAG

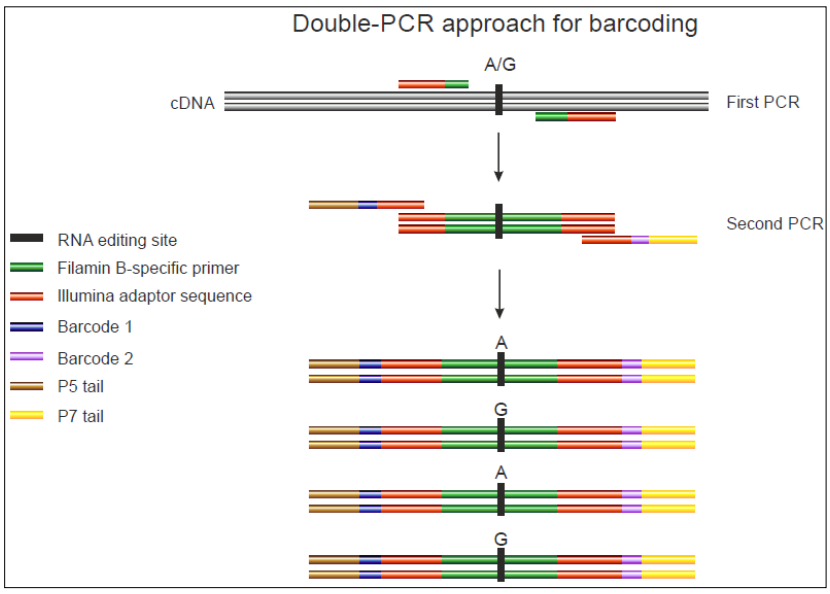

Figure 3: Workflow of the double-PCR approach to generate barcoded amplicons harbouring the Flnb editing site. cDNA was reverse transcribed from RNA obtained from tissues, then amplified with specific primers flanking the editing site of exon 42 in *Flnb* mRNA. These amplicons were further used for the second PCR. Overlapping sequences between the first and second primer pairs allowed us to generate amplicons harbouring the *Flnb* mRNA editing site flanked by Illumina sequencing adaptors at both 5' and 3' ends.

Immunoprecipitation and western blot

Lysis of tissue

Tissues from mice were lysed using approximately 1ml lysis buffer per 50 mg of sample. Right before homogenisation 10x proteinase inhibitor cocktail tablets (Roche 11836170001) were added to the lysis buffer to a final concentration of 1x. 100µl of lysis buffer was added to the tissue and mechanically homogenised with scissors before sonication (4 pulses at 35% of power for twenty seconds. After centrifugation for 30 minutes at maximum speed, the supernatant was transferred to a clean 1.5 ml Eppendorf tube. 5-10% of total lysate was used as input before proceeding with immunoprecipitation. The following steps of the protocol were performed at 4°C. Several lysis buffers were used:

NET-2 buffer: 50mM Tris-HCl pH 7.4, 150mM NaCl, 0,05% NP40

RIPA buffer: 50mM Tris-HCl pH 8, 150mM NaCl, 1% NP40, 0,5% Sodium Deoxycholate, 0,1% SDS

CHAPS buffer: 50mM Tris-HCl pH 7.4, 150mM NaCl, 1% CHAPS, 2mM EDTA

NP40 buffer: 50mM Tris-HCl pH 7.4, 150mM NaCl,1mM MgCl2, 1% NP40, 1mM EGTA

Modified Buffer: 50mM Tris-HCl pH 8, 150mM NaCl, 1% NP40, 2mM EDTA, 10mM $MgCl_2$

Immunoprecipitation

For each immunoprecipitation (IP) 30µl of magnetic beads (Dynabeads®) covalently coupled with Protein A, G or PAN mouse IgG were incubated with antibodies (ABs) specific for mouse FLNA. Both, a polyclonal and a monoclonal antibody (ABs) against repeat 22 of FLNA were used to pull down FLNA (rabbit AB against FLNA from "Biomol Bethyl laboratories, inc." and homemade mouse AB 1B6, 478 and 179, respectively). For the rabbit polyclonal 478 and 479 antibodies we used 50µl for each IP for beads coated with protein A. For 1B6 pull down, 30µl beads coated with protein G were incubated with 50µl 1B6 AB. For the commercial antibody, 2.5µl were added to a total amount of 30µl magnetic beads coated with protein A for every single IP. Binding of these ABs was performed at 4°C while shaking on a rotator overnight. After antibody binding, beads were washed two times with 1xPBS using a magnetic rack. These beads were then incubated in the lysis buffer used for sample preparation.

After removal of an input aliquot, sample lysates were added to the magnetic beads (same amount per run) and incubated on a rotator at 4°C overnight. The inputs were processed in parallel. After washing the magnetic beads three times with 1x TBS (50mM Tris, 150mM NaCl, pH 7.4), 30µl 2x SDS-loading-dye was added and beads boiled at 95°C for 5 minutes. If not otherwise mentioned these samples were directly used and load on an 8% SDS PAGE (polyacrylamide gel electrophoresis).

SDS-PAGE

8% SDS-PAGE gel: 2.5ml 30% Acrylamide (29:1), 3.1ml H20, 3.4ml 1M Tris pH 8.8, 91µl 10% SDS, 91µl 10% APS and 19,5µl TEMED. Stacking gel: 830µl 30% Acrylamide (29:1), 3.4ml H20, 630µl 1M Tris pH 6.8, 50µl 10% SDS, 50µl 10% APS and 5µl TEMED. Glass plates with 1.5mm spacers were used to cast the gel. Samples and ladder (NEB p7712) were loaded on the SDS-PAGE and electrophoresis performed at 80 Volts in 1x SDS-Running buffer. Once the dye reached the separation gel, the voltage was increased to 120 volts.

Western Blot

The separated proteins were transferred on a nitrocellulose membrane from the negative to the positive site, following components were stacked on each other: Sponge, filter, PAGE-Gel, nitrocellulose membrane, filter and a sponge. Transfer Buffer: 25 mM Tris, 192 mM glycine, 20% methanol. Running conditions: 80 Volt for two and a half hours at 4°C.

Detection of Proteins by chemiluminescence

1x Ponceau S staining validated the protein transfer on the nitrocellulose membrane. The membrane was then washed with ultra-pure water, three times with 0,5% milk in TBST and incubated with the primary antibody against FLNA at 4°C overnight while shaking. 1B6 was used as primary AB (1:25 in 0,5% milk in TBST). The membrane was washed three times with 0,5% milk in TBST. The secondary AB anti-mouse-HRP (1:5000 in 0,5mg milk in TBST) incubated for one hour at room temperature while shaking. The membrane was washed three times with 1xTBST. For detection, via chemiluminescence, the “Clarity™ Western ECL Substrate” from BIO-RAD was used. Western luminal/enhancer solution and peroxide solution was mixed 1:1 and added on the nitrocellulose membrane. After an incubation of 5 minutes, the blot was imaged by the Fusion FX system (EvolutionCapt FX6; BIO-RAD).

Tissue culture: human melanoma (M2) cells

Frozen M2 cells stably expressing ether edited FLNA (derived from and labelled as colony 14) or unedited FLNA (colony 100) were thawed quickly. The cells were then transferred to a 15ml falcon tube, and 9ml of fresh media (DMEM, 10% FBS, 1% Penicillin/Streptomycin, 2nM L-Glycine) was added. After spinning for 3 minutes at 1000 rpm, the supernatant was removed to get rid of DMSO. Ten millilitres of media were added to resuspend the pellet and cells were seeded on 10mm dishes. After one day of recovery, 100µg/ml Hygromycin B (100mg/ml) was added to select for M2 cells harbouring edited or unedited FLNA.

M2 edited and unedited cells that showed a confluence of about 80% were used to perform foci formation and proliferation assays.

Proliferation assay

For each M2 cell line (edited and unedited) cells were seeded in triplicate at a density of $3x10^5$ cells per 3 cm dish. Hygromycin B was added accordingly. After 24, 48, 72 and 96 hours cells were counted using the Countess II FL Automated Cell Counter (Invitrogen).

Foci assay

For each M2 cell line (edited and unedited) cells were seeded at a density of 100 or 250 cells per 3 cm dish. Hygromycin B was added accordingly. After 6-8 days cells were washed, fixed and stained. Crystal Violet Cell Colony Staining (1 L): 0.5 g Crystal Violet (0.05% w/v) 27 ml 37% Formaldehyde (1%) 100 mL 10X PBS (1X) 10 mL Methanol (1%) and 863 dH_20. Foci were counted with ImageJ software.

Results

Spatio-temporal profiling of Filamin B RNA-editing in mouse

Table 2: List of tissues extracted from newborn (P0), Juvenile (P21) and adult (P120) mice.

Newborn	Juvenile	Adult
Cartilage (ribs)	Cartilage (ribs)	Cartilage (ribs)
Femur	Femur	Femur
Bladder	Bladder	Bladder
Heart	Heart	Heart
Lung	Lung	Lung
Stomach	Stomach	Stomach
Skeletal muscle	Skeletal muscle	Skeletal muscle
Liver	Liver	Liver
Skull	Skull	Skull
Cerebellum	Cerebellum	Cerebellum
Skin	Skin	Skin
Cortex	Cortex	Cortex
Small intestine	Small intestine	Small intestine
Kidney	Kidney	Kidney
Large intestine	Large intestine	Large intestine
Spleen	Spleen	Spleen
Eye	Eye	Eye
Blood	Blood	Blood
	Cartilage (kneecap)	Cartilage (kneecap)
	Spinal cord	Spinal cord
	Testis	Testis
	Olfactory bulb	Olfactory bulb
	Visceral fat	Visceral fat
	Aorta	Aorta

Primers for mRNA of *Flnb* editing site amplification were designed on two different but consecutive exons of *Flnb* mRNA, exon 42 and 43 and tested on cDNA reverse-transcribed from total RNA. PCR products were then loaded and run on a 2% agarose gel (figure 4), cut out and eluted in water by using silica matrices. The concentration was measured by UV absorption and the right amount of amplicon sent for Sanger sequencing with the reverse primer.

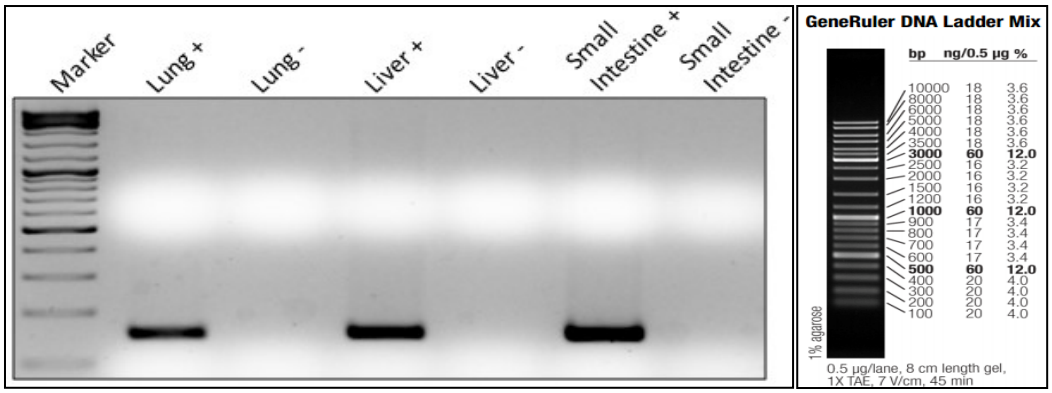

Figure 4: PCR products for *Flnb* mRNA. PCR samples from different tissues were run on a 2% agarose gel. No sign of contamination is evident in the RT$^-$-PCR samples.

After the primer specificity was confirmed, fresh mouse tissues were isolated. Tissues were collected and immediately frozen in liquid nitrogen. If not used immediately, samples were stored at -80°C. For RNA extraction commercially available kits were used following the enclosed instructions ("PerfectPure^{tm} RNA Cell & Tissue" from 5Prime or "E.Z.N.A.® Tissue RNA Kit" from Omega Bio-Tek). The RNA yield of the two kits was compared on agarose/formaldehyde gel (figure 5). The peq GOLD TriFast™ reagent (see Material and Methods) was used for processing further samples. Since the DNase I digestion step was included in both kits, reverse transcription was performed directly after RNA elution. An additional DNase I digestion step (see Material and Methods) was performed the peq GOLD TriFast™ reagent was used to extract RNA.

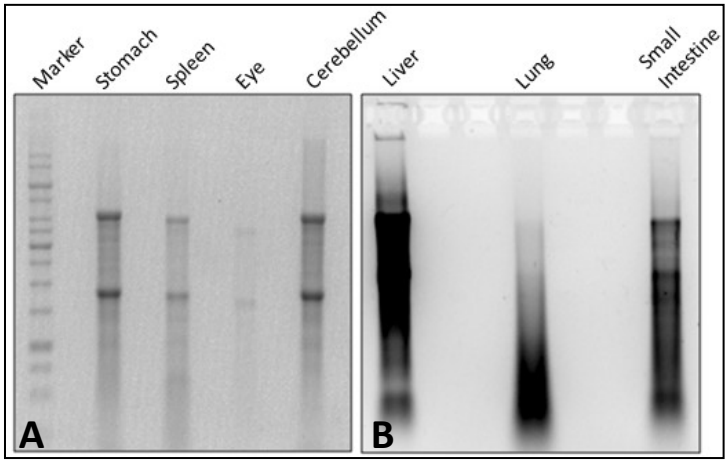

Figure 5: Comparison of the kits used for RNA extraction. Agarose/formaldehyde gel for RNAs extracted from different organs of P120 wt mouse with the PerfectPure^{tm} RNA Cell & Tissue kit (A) and the E.Z.N.A.® Tissue RNA Kit (B). Total RNA quality varies depending on the extraction kit used.

The amplification of the specific editing site for *Flnb* mRNA was performed by PCR on reverse transcribed cDNA. For every reverse transcription (RT$^+$-PCR) a negative control (RT$^-$-PCR) was processed in parallel by adding DEPC water instead of the RT enzyme (figure 4). This allowed us to check for possible contaminations in our extracted RNA samples. The amplification product has an expected length of 148 nucleotides. PCR products of the correct size are shown

in figure 4. Only samples showing no product in the corresponding RT-PCR reaction were further processed. Examples of contaminated samples are shown in figure 6.

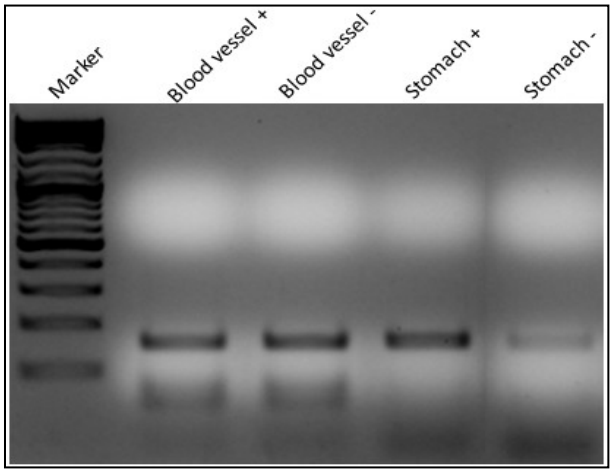

Figure 6: Example of contaminated PCR reactions. PCR samples from different tissues were run on a 2% agarose gel. Samples are showing bands of the expected size also in RT-PCR samples were discarded.

Amplified bands were sent for sequence verification by Sanger sequencing (Eurofins pickup service), comprising few samples from the previous *Flna* study (Stulic and Jantsch, 2013).

The Sanger sequencing results were analyzed by FinchTV, Chromas or Geneious software packages. The percentage of edited Flnb mRNA was measured from the height of the peaks in the chromatograms with the following formula: $\left(\frac{Hc}{Hc+Ht}\right) * 100$, where Hc is the height of the edited nucleotide peak and Ht is the height of the unedited nucleotide peak.

Initially, only the *Flnb* mRNA editing level in lung and muscle could be compared between mice of different ages (figure 7). *Flnb* editing levels are elevated in skeletal muscle, cerebellum, liver and eye reaching almost 40% editing or more. *Flnb* mRNA editing level in muscle increases from P0 to P21, following the same trend of in *Flna* editing (Stulic and Jantsch, 2013). In the lung, Flnb RNA editing does not change between P0 and P21 mice.

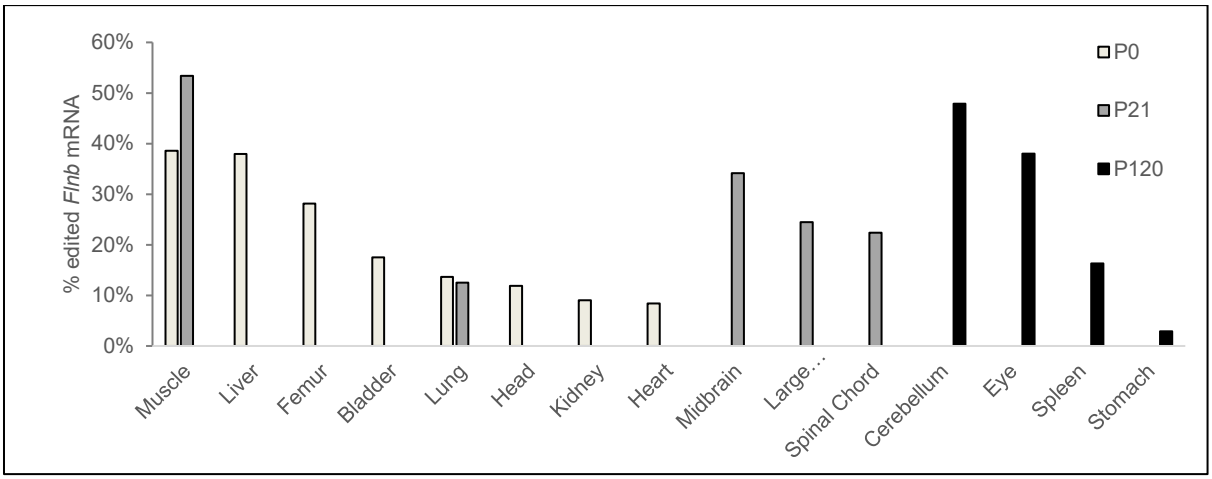

Figure 7: Flnb editing levels measured by Sanger sequencing. Percentage of editing levels in *Flnb* mRNA in the neonate (P0), juvenile (P21) and adult (P120) wild-type mice are shown.

To profile Flnb editing by next-generation sequencing (NGS), we designed a double PCR approach. To obtain a short amplicon harbouring the Flnb editing site we designed a forward primer on exon 42 and a reverse primer on exon 43, both harbouring a portion of the sequencing adaptor as an overhang. For the second PCR indexed i7 and i5 primers that specifically bind to the adaptor sequence introduced in the previous PCR were used (NEB Next® Multiplex Oligos for Illumina® (Dual Index Primers Set 1)). The provided eight nucleotide-long barcodes on the 5' (i5) and 3' (i7) ends of the final amplified products allowed us to distinguish samples by tissue of origin and mouse age.

To preserve the balance of edited and unedited *Flnb* mRNA per sample, we aimed at reducing the number of amplification cycles during PCRs to a minimum. The first PCR was run with fifteen cycles. The second PCR was performed with twenty fife cycles. After the first PCR with 15 amplification cycles, the product was extracted without gel purification. One-third of the first PCR product was used for the second indexing PCR. After a total of 40 cycles, the barcoded PCR products were visible on an agarose gel (figure 8).

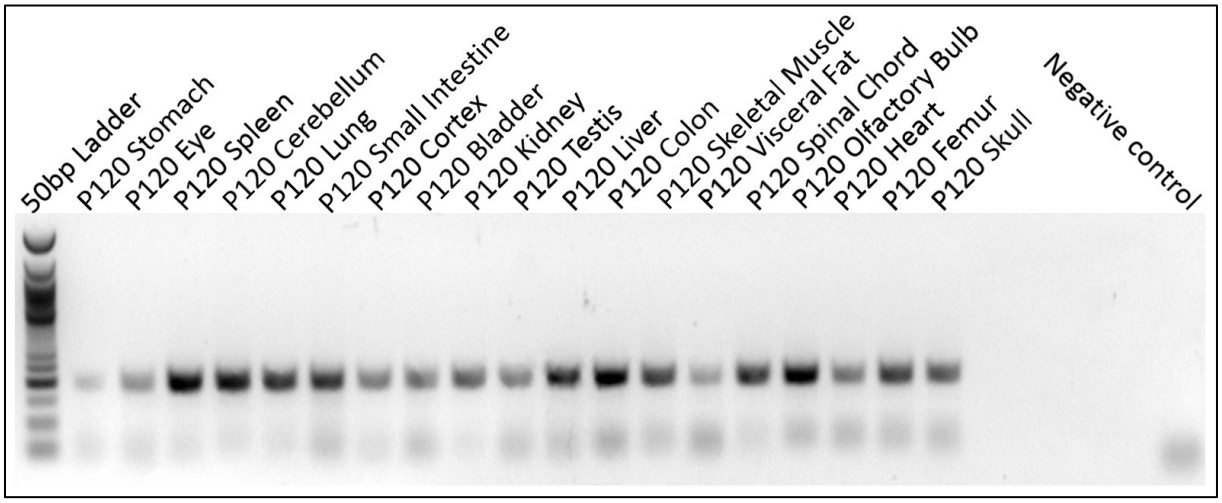

Figure 8: **Indexed *Flnb* amplicons.** The expected length of the amplicon harbouring Flnb editing site is 194bp. In addition to the Flnb mRNA amplicon (58 bp), PCR products contain Illumina adaptor (33 bp at the 5' end and 34 bp at 3' end) and barcoding sequences (29bp at the 5' end and 24bp at the 3' end). Electrophoresis was performed in a 2% agarose gel.

Bands at the expected size were cut out, gel-extracted using silica matrices and eluted in water. The amplicon sequence was validated by Sanger sequencing of few random samples (figure 9). Concentrations were measured by fluorometer and 10ng of each sample were pooled and concentrated by using a silica matrix. By the VBCF (Vienna Biocenter Core Facilities) pooled samples were checked qualitatively by fragment size analysis and quantitatively by quantitative PCR before being processed for Illumina sequencing (fig. 10).

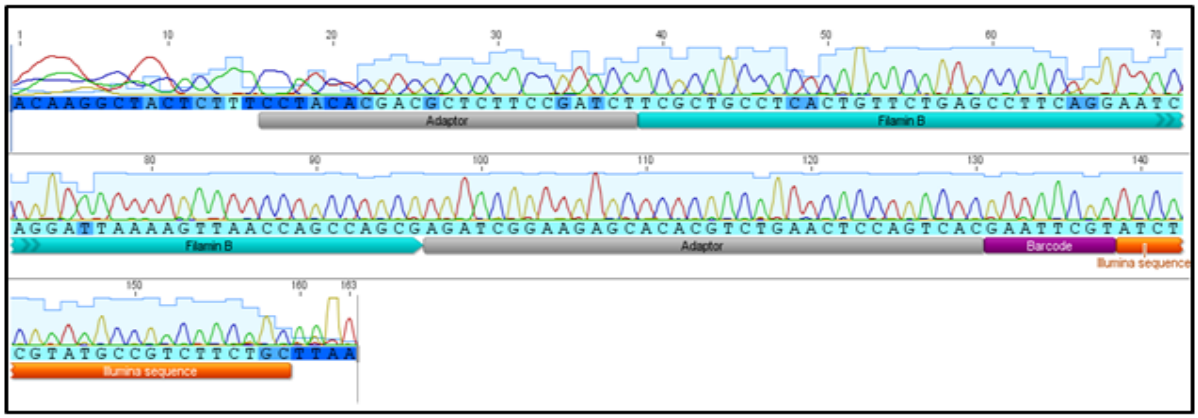

Figure 9: Randomly picked double barcoded samples were checked by Sanger sequencing. Here, the chromatogram of spleen at P21 is shown. Correct barcode sequences were identified in all tested samples. Grey: Adaptor sequence; Blue: *Flnb* cDNA sequence; Purple: Barcode sequence; Orange: Illumina primer sequence.

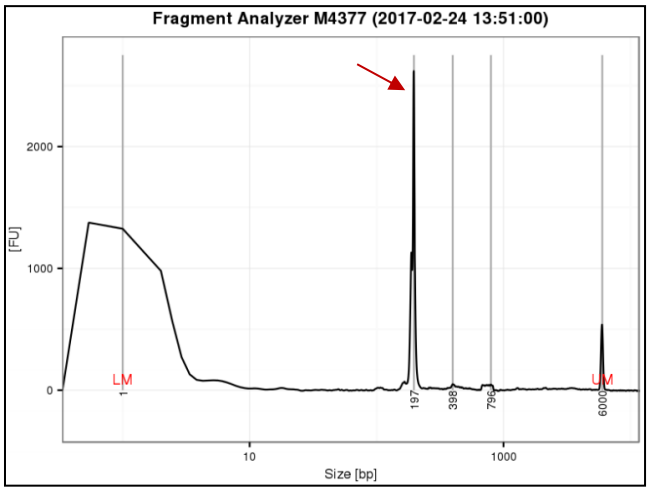

Figure 10: Results of the fragment analyser performed by VBCF. Pooled fragments of the barcoded amplicons can be seen at the 197 base-pair peak (arrow) at the expected length.

On an Illumina 2500 machine, 50 base pairs downstream of the 5' Illumina adaptor were sequenced. Biological replicas of organs and time points yielded 1.49 million reads. The average read count is 7,450 reads per sample. The number of reads varied from a maximum of 7,990 reads to a minimum of 247 reads per sample.

Sequencing quality was assessed in every sample. Even at the lowest coverage, the observed background sequencing error rate - in the range of one-tenth of a percent did not affect the quantification of editing rates. All reads were aligned to the mRNA reference sequence of *Flnb* containing the specific editing site. For each combination of indexes, the percentage of edited Flnb transcripts was calculated. A small percentage of reads did not perfectly align to the reference *Flnb* sequence but due to errors aroused from primer irregularity. In femur (long bone), skull (flat bone), cartilage, aorta, blood, heart, skeletal muscle, visceral white fat, skin

and cerebellum Flnb editing exceeded 50% in at least one of the developmental time points (figure 11). In each developmental stage, these tissues are amongst the highest edited tissues. Levels of editing between 25-50% were found in olfactory bulb, cortex, eye, spleen, liver and lung. Low editing levels could be detected in the small and large intestine, spinal cord, lung, testis, kidney and bladder.

In bladder, spleen, small intestine and aorta a decrease in editing over time are shown. In four tissues the Flnb editing drops in juvenile mice (stomach, large intestine, lung and liver). Instead, in blood and ribs (cartilage), it appears that Flnb editing reaches its peak in juvenile mice and slightly drops in adulthood. Nevertheless, in general, Flnb editing increases during post-natal development (in 14 out of 22 organs). This increase is evident in most of the tissues with elevated editing, for example in bone (skull and femur), cerebellum or skeletal muscle.

It is worth mentioning that in some tissues, the difference of editing between biological replicates varies drastically, as can be seen in the standard deviation (Table 3).

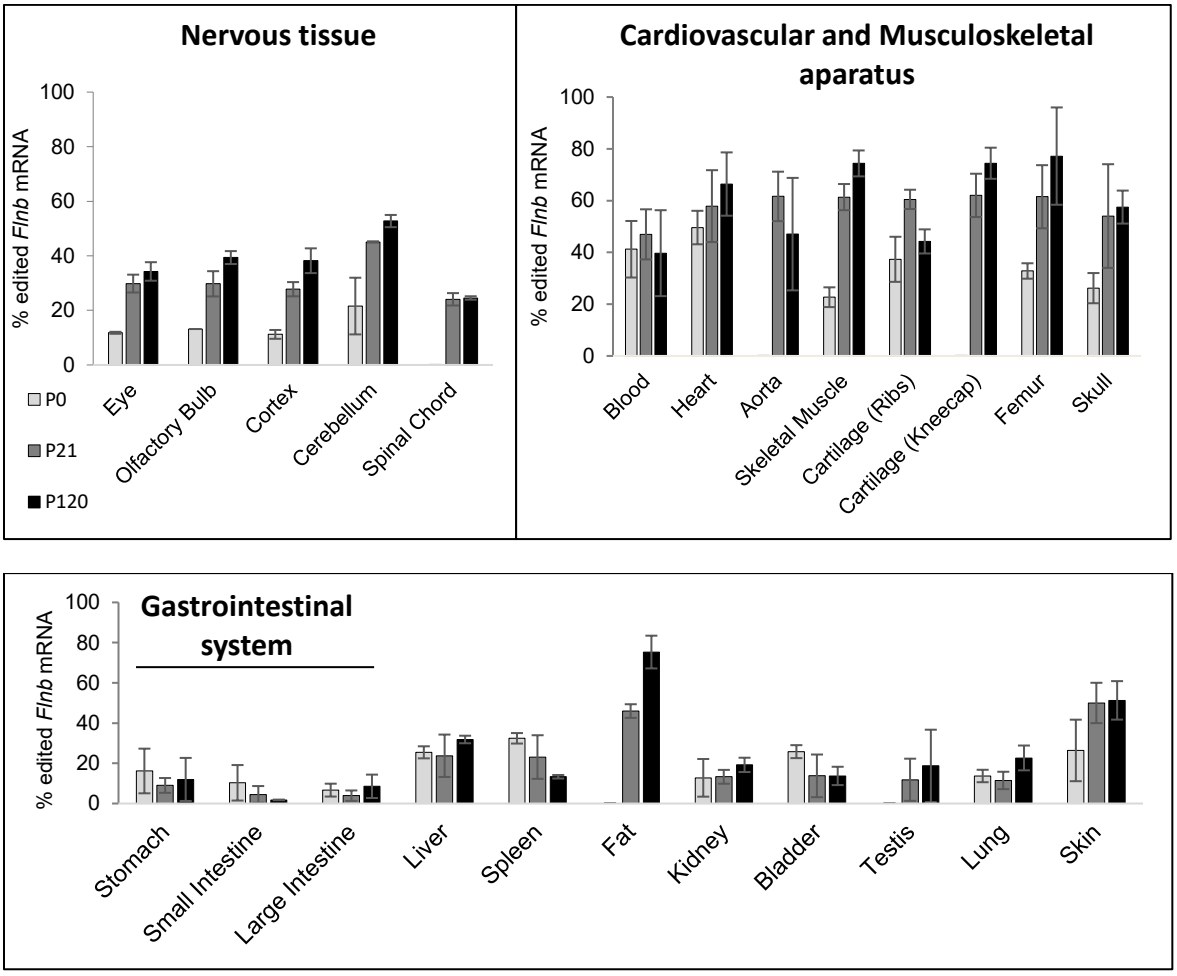

Figure 11: *Flnb* A-to-I editing rates at the Q/R site in wild-type mice. The proportion of edited Flnb mRNA in mouse tissues at birth (P0), 21 and 120 days after birth (P21 and P120, respectively). Flnb editing increases with age and the highest editing levels are detected in the cardiovascular and musculoskeletal apparatus (top right panel). Data are plotted as mean ± standard deviation.

At the Flnb Q/R editing site, neonate mice show editing above 30% in blood, heart, cartilage, femur and spleen. Lowest levels of editing can be seen in eyes, cortex, olfactory bulb, kidney, large and small intestine showing editing of around 15% or lower. The remaining tissues exhibit editing between 15-30%.

By looking at the spatio-temporal editing levels in the twenty-one-day old mice we were able to detect the highest editing of *Flnb* mRNA in bones, heart, aorta, skeletal muscle and cartilage. These tissues have an average editing level higher than 50% and a maximum of about 62% in the kneecap. Intermediate editing levels are found in eyes, olfactory bulb, cortex, cerebellum, blood, fat and skin, ranging from 27-47% respectively. Editing in the spinal cord, stomach, liver, spleen, kidney, bladder, testis, lung, the large and small intestine is low and reaches a maximum of 24% and a minimum of about 4% in the large intestine.

Highest editing was found in adult mice. Up to 75% editing is found in fat, skeletal muscle, cartilage (kneecap) and femur. Intermediate levels of A-to-I editing of over 50% can be seen in cerebellum, heart, skull and skin. Moderate editing between 30% and 50% takes place in the eyes, olfactory bulb, cortex, blood, aorta, cartilage (ribs) and liver. Remaining tissues show editing below 30% with large intestine, small intestine, spleen and bladder showing the lowest editing.

Editing of FLNB has been reported to undergo circadian cycles. We, therefore, compared Flnb editing levels from tissues isolated early in the morning when Flnb editing is expected to be elevated in the afternoon (figure 12). However, a general trend in higher editing in the morning hours was not detected. Instead, editing seems to be similar between tissues obtained in the morning and the afternoon.

Table 3: Editing at the Q/R site of Flnb across mouse tissues during post-natal development. Editing levels are calculated for each tissue as the average of biological replicas**.**

P0 Tissues	% Flnb editing	StdDev
Eye	11,79	0,36
Olfactory Bulb	13,17	--
Cortex	11,20	1,62
Cerebellum	21,58	10,39
Spinal Chord	--	--
Blood	41,21	10,92
Heart	49,59	6,47
Aorta	--	--
Skeletal Muscle	22,69	3,82
Cartilage (Ribs)	37,33	8,70
Cartilage (Kneecap)	--	--
Femur	32,82	2,98
Skull	26,19	5,83
Stomach	16,19	11,10
Small intestine	10,30	8,82
Colon	6,66	3,20
Liver	25,45	3,00
Spleen	32,42	2,60
Visceral Fat	--	--
Kidney	12,78	9,36
Bladder	25,80	3,22
Testis	--	--
Lung	13,69	3,09
Skin	26,40	15,29

P21 Tissues	% Flnb editing	StdDev
Eye	29,83	3,27
Olfactory Bulb	29,74	4,63
Cortex	27,76	2,60
Cerebellum	45,08	0,23
Spinal Chord	24,06	2,27
Blood	46,96	9,68
Heart	57,88	13,88
Aorta	61,62	9,55
Skeletal Muscle	61,36	5,05
Cartilage (Ribs)	60,48	3,72
Cartilage (Kneecap)	62,02	8,36
Femur	61,50	12,20
Skull	54,04	20,03
Stomach	9,00	3,68
Small intestine	4,51	4,17
Colon	3,90	2,60
Liver	23,75	10,54
Spleen	23,11	10,84
Visceral Fat	45,98	3,39
Kidney	13,29	3,44
Bladder	13,76	10,61
Testis	11,82	10,48
Lung	11,47	4,33
Skin	50,00	10,03

P120 Tissues	% Flnb editing	StdDev
Eye	34,26	3,40
Olfactory Bulb	39,36	2,37
Cortex	38,20	4,53
Cerebellum	52,74	2,24
Spinal Chord	24,56	0,62
Blood	39,71	16,60
Heart	66,40	12,23
Aorta	47,05	21,73
Skeletal Muscle	74,37	5,01
Cartilage (Ribs)	44,24	4,66
Cartilage (Kneecap)	74,44	6,01
Femur	77,20	18,80
Skull	57,50	6,37
Stomach	11,98	10,70
Small intestine	1,81	0,14
Colon	8,55	5,82
Liver	31,84	1,88
Spleen	13,31	0,87
Visceral Fat	75,31	8,14
Kidney	19,22	3,56
Bladder	13,72	4,56
Testis	18,70	18,00
Lung	22,67	6,16
Skin	51,29	9,57

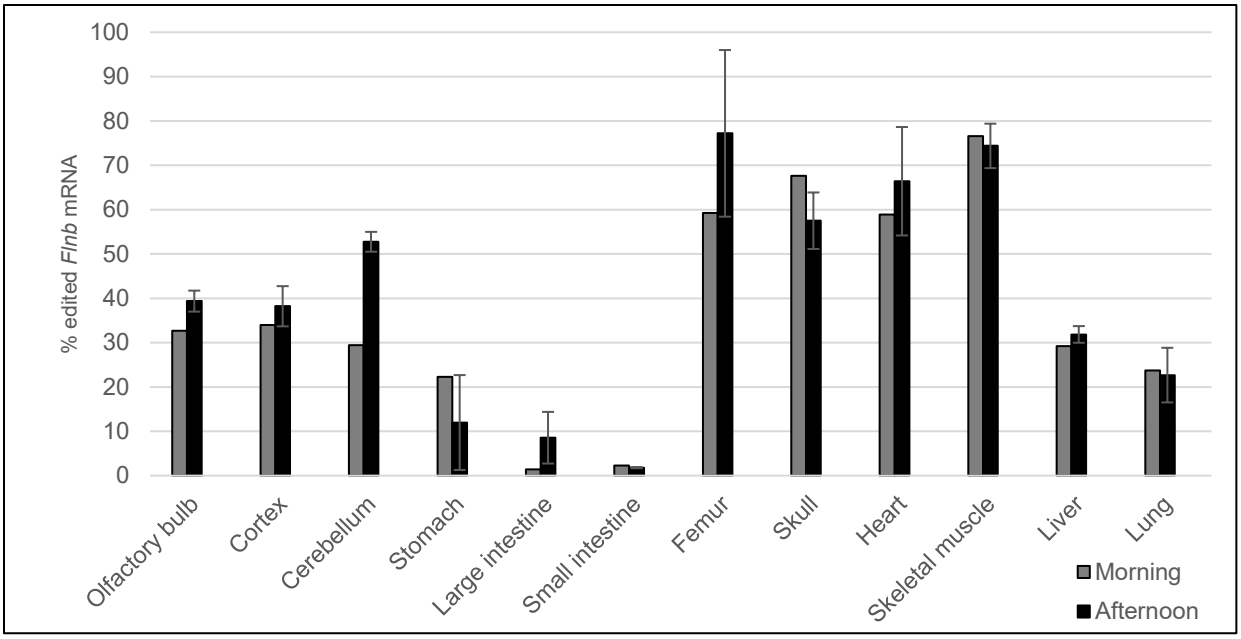

Figure 12: Comparison of Flnb editing levels in the morning and the afternoon. Black bars show samples harvested in the afternoon; grey bars show tissues harvested in the morning. Twelve organs of one mouse were compared to the average editing levels of tissues obtained in the afternoon to get a general overview of the circadian profile of Flnb editing.

Human melanoma cell assays

Aberrant editing is displayed in various cancerous tissues. We hypothesise that increased expression of edited Filamin A protein reflecting hyper editing may influence tumour formation. To test if the editing in the coding sequence of this protein has an effect on malignancy we performed first subsequent assays to address this question in human M2 cell lines.

The following proliferation and foci assays were performed on human melanoma M2 cell lines since these cells lack Filamin A expression and are therefore ideal for transfection of desired Filamin A constructs. Human M2 cells were stably transfected with either unedited or edited *Flna* cDNA (referred to as unedited M2 and edited M2, respectively) where the expression vector harbours a hygromycin resistance for selection.

To test the effect of Flna editing on cell proliferation, cells were seeded in equal amounts. At 24, 48, 72 and 96 hours post seeding cells were counted to compare their proliferation rate. Figure 13 represents the cumulative data of two replicas. A statistically significant increase in proliferation was detected at day 4 for M2 cells expressing edited Flna.

With the foci assay, the growth potential of single cells can be tested. Carefully translated into the field of oncology, this assay tests the malignancy ability of cells. We seeded the same number of cells for each M2 cell line and let them grow for more than five days to obtain visible colonies/foci. Cells were then fixed, stained, imaged and counted (figure 14).

As seen in figure 14, M2 cells replenished with unedited *FLNA* form significantly more colonies compared to M2 cells with edited *FLNA* at all seeding densities and for all technical replicas. With such a detected difference, we questioned how the structural appearance of the foci differs between those two cell lines. Therefore, representative colonies were imaged at higher magnification and compared. As shown in figure 15, foci show a clear difference in size: edited M2 foci appeared bigger and denser than the foci formed by unedited M2.

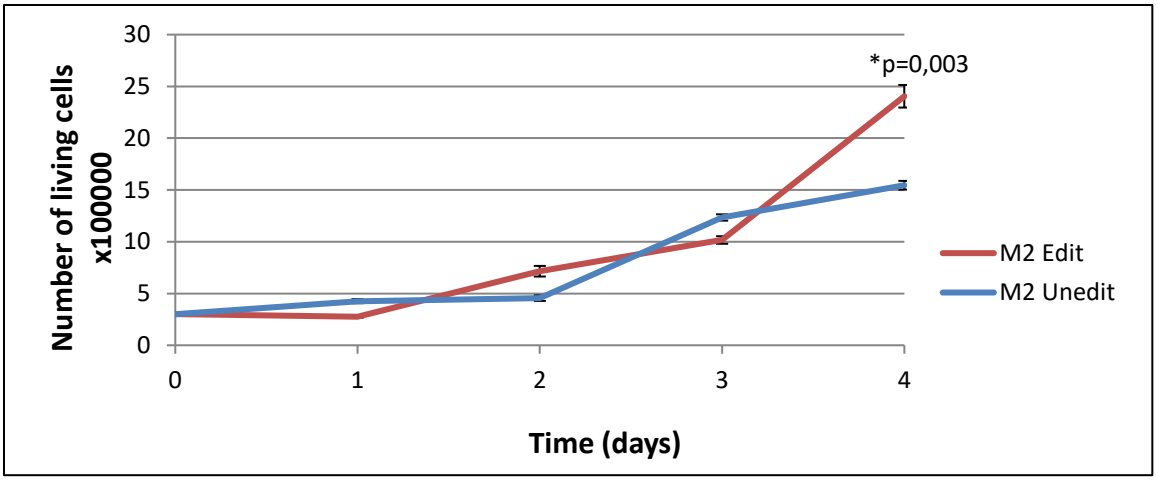

Figure 13: Proliferation assays of edited and unedited M2 cells. Starting with an equal number of seeded cells, M2 cells replenished with either edited or unedited Flna were counted at different time points. After four days in culture edited M2 cells show a significant increase in cell number. The combined data of two replicas are plotted as mean ± s.d.

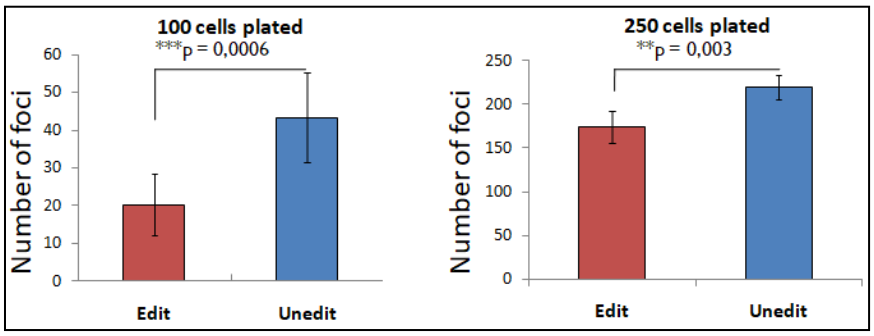

Figure 14: Foci forming potential of edited and unedited M2 cell lines. Cells were seeded at a density of either 100 (A and C) or 250 (B and D) seeded cells/dish. After seven days a larger number of foci was observed for cells harbouring unedited FLNA.

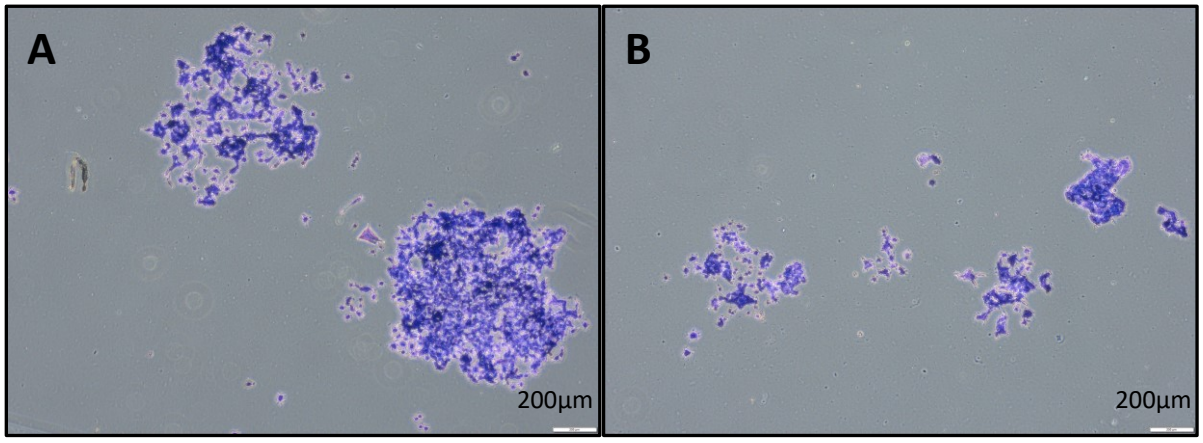

Figure 15: Foci formed by stably transfected M2 cells imaged on a bright field microscope. (A) Foci formed by M2 replenished with edited *FLNA*(A) or unedited *FLNA* (B) after eight days in culture.

We checked for editing by Sanger sequencing to make sure that both cell lines (clone 14 and 100) are edited accordingly (figure 16 D). Also, to be sure that both cell lines still express the introduced FLNA, FLNA expression was analysed by immune fluorescence and western blot taking advantage of the myc-tag introduced at the C-terminal of introduced *FLNA* cDNA sequences (figure 16 A, B and C). As shown the edited clone number 14 that was used for the assays suffered a significant loss of FLNA expression when compared to clone 8. The same applies to the unedited clone number 100 which was compared to the clone number 127.

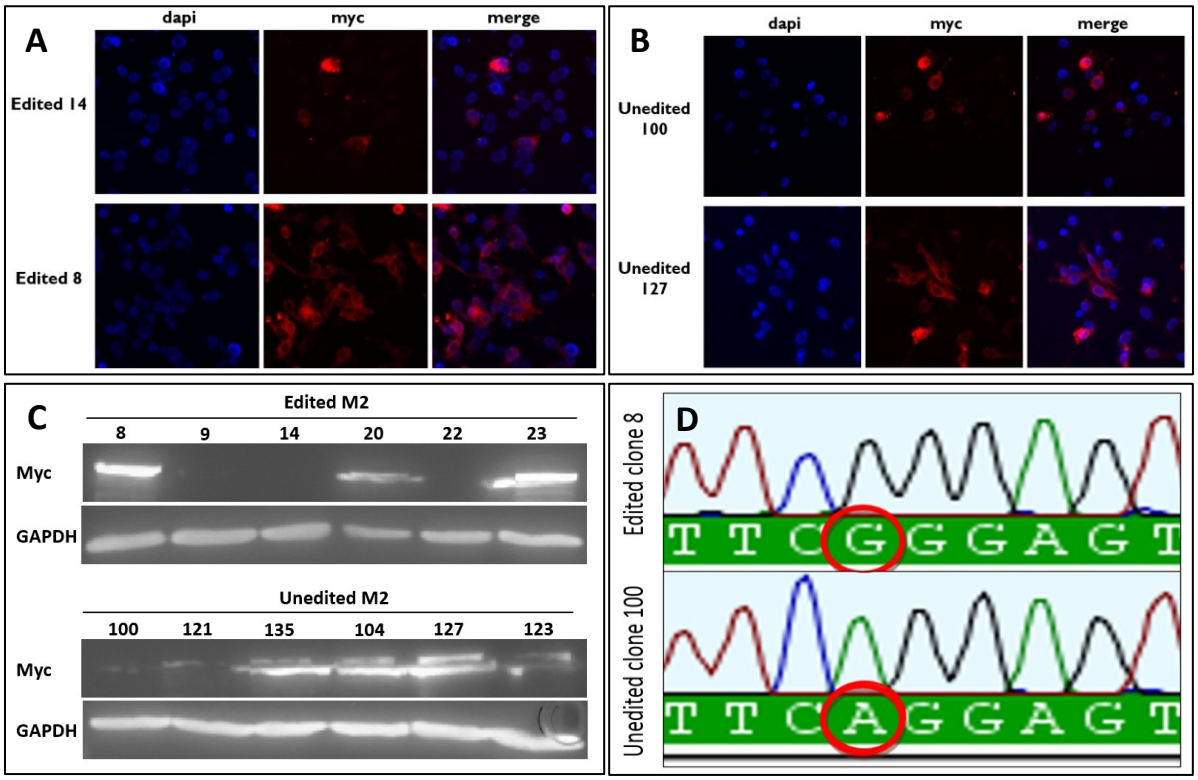

Figure 16: Immunofluorescence of M2cell lines stably transfected with edited or unedited myc-tagged FLNA constructs. (A) Expression of edited FLNA in clones 14 and 8. (B) Expression of unedited FLNA in clones 100 and 137. (C) Western blot analysis with antibodies again GAPDH and Myc of all the M2 colonies transfected with Flna cDNA plasmids. All clones were tested for Myc-FLNA expression and compared to GAPDH expression levels. (C, Top) Myc-FLNA and GAPDH expression of M2 edited cells (14) used in our assays are seen in the third column. (C, Bottom) Unedited M2 cells (100) used in our experiments and corresponding Myc-FLNA and GAPDH expression levels are visible in the first column. (D) Chromatograms of M2 cells replenished with edited or unedited Flna. (D, Top) M2 cells transfected with Flna cDNA mimicking a fully edited state. (D, Bottom) M2 cells transfected with Flna cDNA mimicking a fully unedited state.

Table 4: Densitometric analysis and quantification of FLNA expression using the ImageJ software.
Quantification between M2 clones edited 14, 8 and unedited 100 and 127 were performed. Data was retrieved from western blot of cell lysates labelled against GAPDH and Myc-FLNA (figure 19 C). The ratio of GAPDH to Myc expression indicates drastic loss of FLNA expression in Clone 14 and 100.

	Intensity units by ImageJ		
Clone	**GAPDH**	**Myc**	**GAPDH/Myc**
Edited 14	9117,34	747,19	0,08
Edited 8	10073,17	9596,77	0,95
Unedited 100	13168,55	381,02	0,03
Unedited 127	20605,84	13359,38	0,65

Filamin A immunoprecipitation from mouse colon

The goal of establishing a protocol to immunoprecipitate FLNA protein is to identify its binding partners. Ultimately, by precipitation of edited and unedited FLNA, we aim to pinpoint which proteins prefer to bind to either edited or unedited FLNA, giving us hints on how a single editing event can affect the FLNA interactome.

First, different FLNA antibodies were tested by western blotting on total lysates obtained from wild-type mouse colon that was homogenised in NET-2 lysis buffer. As shown in figure 17, all antibodies seemingly recognise FLNA at an expected molecular weight of ~260 kDa. The two, homemade polyclonal antibodies 478 and 479 showed an additional band at ~200kDa, a potential breakdown product of FLNA. The home-made monoclonal 1B6 antibody gives a signal comparable to that of the commercial antibody at the expected molecular weight of ~260 kDa and an additional band at 90kDa. Next, several lysis buffers were tested for tissue homogenization. As shown in figure 18 our homemade lysis buffer modified from the NP40 composition extracts the highest amount of soluble FLNA.

Since we had difficulties getting a clean control of beads without antibody, we started to test four different conditions for the pull-down (table 5). These four conditions varied in the amount of antibody and lysate used. Also, the incubation time for the pull-down varied from one to two hours. In condition one and two we used same amounts of 1B6 AB (300µl) and lysate (600µl) for the pull-down. In condition one, beads with 1B6 and lysate were incubated for one hour, and in condition two we increased the time to two hours. In the conditions three and four, we used 500µl of 1B6 AB and incubated for two hours in both conditions. In condition three we used 500µl lysate compared to 300µl in condition four. By optimising the conditions of the FLNA pull-down, we were able to find the best circumstances for a FLNA pull-down and a clean control in condition one (figure 19). These results could not be replicated due to lack of time.

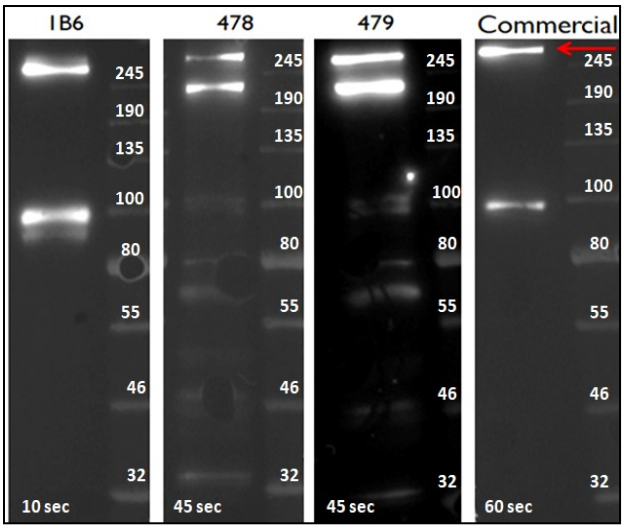

Figure 17: Different antibodies against FLNA were tested. Colon tissues from wild-type mouse were lysed in NET-2 buffer, and FLNA was visualised from the lysate by home-made monoclonal 1B6, home-made polyclonal 478 and 479, or commercial antibodies. The different exposure times are marked at the bottom. The red arrow indicates FLNA expected molecular weight. White numbers indicate the molecular weight of the marker.

Table 5: Conditions tested to find the ideal FLNA pull-down condition. Four conditions were tested. A varying amount of total lysate, 1B6 antibody and the incubation time provided us with the best option for the FLNA pull down. Each condition was different in at least one factor compared to other conditions. For the 1B6 antibody dilution used see material and methods.

	Total lysate	Antibody 1B6	Incubation time
Condition 1	600µl	300µl	60 min
Condition 2	600µl	300µl	120 min
Condition 3	500µl	500µl	120 min
Condition 4	300µl	500µl	120 min

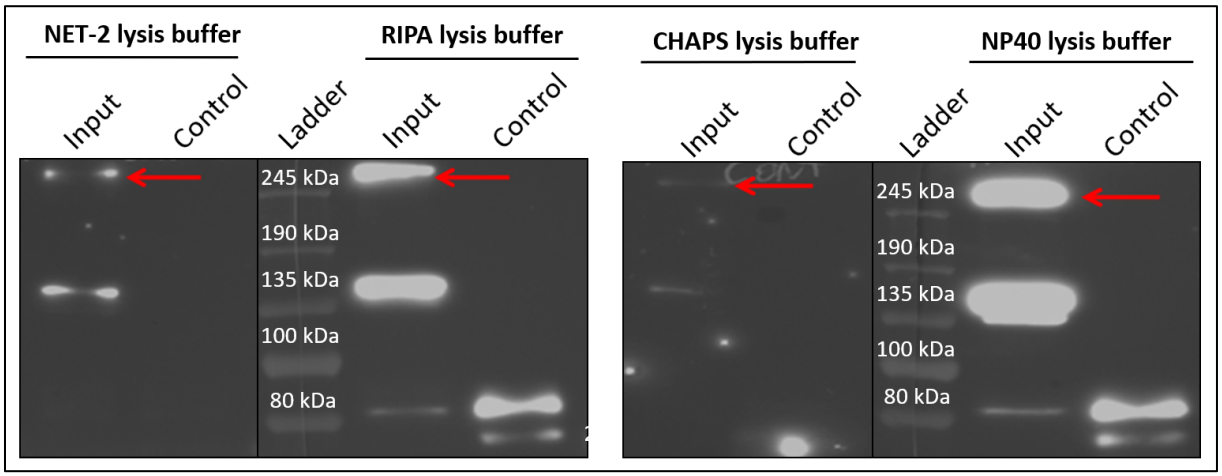

Figure 18: Immunoprecipitation of FLNA from the colon with the 1B6 antibody. Colon tissues were lysed in different buffers, and FLNA was visualised with the 1B6 antibody. Exposure time = 5'. The red arrow indicates FLNA expected height/molecular weight.

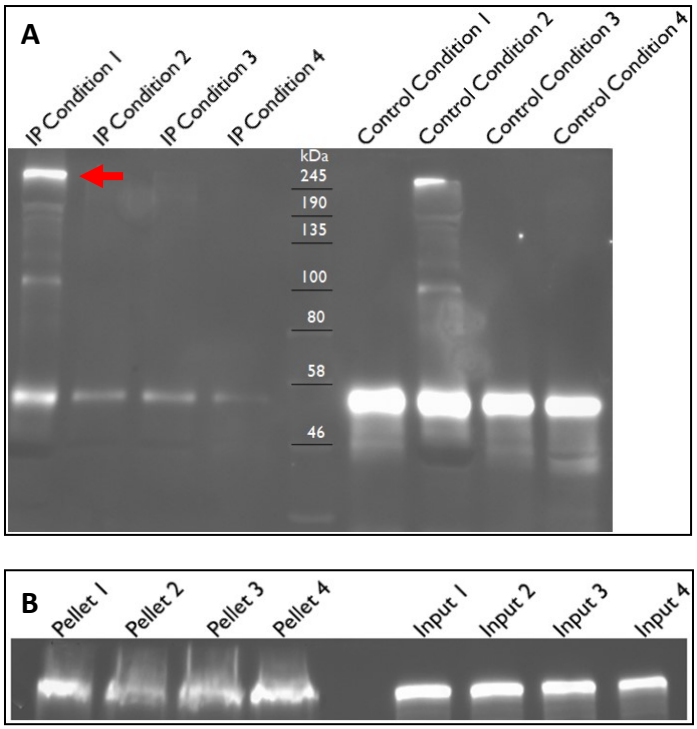

Figure 19: Immunoprecipitation of FLNA from mouse colon. (**A**) Colon tissues were lysed in our modified buffer. FLNA was immunoprecipitated and visualised with the 1B6 antibody. Exposure time = 1'. (**B**) SDS loading dye was directly added to the tissue pellet after recovery of the lysate to check the quantity of FLNA which is not recovered with the lysis. Input percentage loaded ranged from 3,3 to 6,6% depending on the condition (see material and methods). The red arrow indicates FLNA expected molecular weight.

Discussion

In 2013 a study was performed by the Jantsch group where *Flna* mRNA editing levels in wild-type and *ADAR2* knockout mouse models were analysed (Stulić and Jantsch 2013). We started a slightly different new approach for *Flnb* mRNA editing measurement by the two-step PCR approach for barcoding amplicons that were collected from adult, juvenile and newborn wild-type mice for next-generation sequencing.

By amplifying a short region around the editing site of *Flnb* mRNA that resides at the end of exon 42, we were able to assess the quality of tissue-extracted RNA samples and judge them suitable for NGS. Samples that showed bands in the negative (RT^--PCR) control were discarded. Likely, these negative controls got contaminated during pipetting and/or processing of several samples simultaneously. Appropriate precautions were taken to avoid contaminations after which the RT^- controls showed no bands (fig. 2).

More tissues had to be processed to create a bigger library of samples to approach NGS. By designing new primers closer to the editing site, we were able to obtain shorter PCR products which are suitable for further NGS library preparation. We decided to a double-PCR-approach for barcoding and adaptor addition. Following the double-PCR-approach, the first set of primers were designed with overhangs complementary to the adaptor sequence at the 5'-end. Then we further amplified the short amplicon with barcoded primers. Amplification cycles were set low, keeping in mind that overamplification may lead to a shift of overrepresented states of adenines/inosines. Furthermore, a representative pool of the first amplicon was taken for the second PCR for the same reason, one third respectively. With a set of twelve different barcodes for the 5'-end and eight different barcodes for the 3'-end which anneal on the adaptor sequence, we were able to label every tissue and time point with a unique combination of 5' and 3' barcodes in the second PCR step. This approach allowed us to pool all samples prior to NGS and still distinguish them during the following NGS data analysis. This approach displays a fast and easy protocol to create an amplicon library for NGS that solely relies on the ability of primer design.

FLNB plays an important role in bone/cartilage development as it has been shown in knockout mice. Although the direct effect or regulation of editing on bone development is not clearly understood. We expected to see high editing or at least an increase over time in bone and cartilaginous tissues. Since newborn mice still need to develop bones and must undergo ossification we expect to see a change in editing between the newborn and juvenile developmental state. Indeed, we see that bone and cartilaginous tissues are amongst the organs exhibiting the highest editing rates (figure 11). Interestingly, we could also detect elevated editing above 60% in aorta, skin, heart, skeletal muscle and visceral fat. Filamins are also proven to have an importance in brain development. In the *Flna* mRNA, only moderate editing of up to 38% in adult mice was seen in the brain. In contrast, *Flnb* editing levels reached over 50% in the brain. Thus, for *Flnb* mRNA editing, we could detect different trends that differ from *Flna*.

Data retrieved from NGS revealed fascinating insights in editing levels of *Flnb* mRNA during development. Especially in the cardiovascular and locomotion system, we see high editing of up to ~75% in the femur, the kneecap and in skeletal muscle, respectively. It has been shown that ADARs are highly active in brain tissues. In our data set, A-to-I editing in brain displays only moderate editing of *Flnb* mRNA demonstrating that some targets have highest editing levels outside the nervous system.

While Flnb editing is highest in cartilaginous tissues, *Flna* mRNA shows elevated editing in the lung, bladder, large intestine and aortic arch in adult mice (Stulic and Jantsch, 2013). Conversely, in tissues with high Flna editing is low in bone and cartilaginous tissues. It is also interesting to note that we could detect higher editing (up to 77%) in tissues that show severe phenotypes in *FLNB*$^{-/-}$ mice suggesting that editing may be crucial to proper FLNB function.

Editing increases during development and may be necessary and characteristic for proper function of organs as recent data showed the involvement of *Flna* mRNA editing in hypercontraction of smooth muscle cells (Jan et al., in press). The same principle may be applied to *Flnb* where editing may be needed for proper development, function and integrity of these organs. Studies on *FLNA* show that mechanical force/stress may expose usually unexposed areas of filamins to potential binding partners or modifying enzymes (Chen et al., 2009). This fact together with the changes in amino acids due to editing in bones/muscles may contribute to a specialised cellular mechanism specific for the musculoskeletal system to deal with this type of stress and/or the development of tissues being part of this system. Therefore, editing in these tissues might increase the specificity of binding to proteins involved in modulating shape, movement or the response to mechanical stress. Nevertheless, further experiments must be performed to test this hypothesis. Today's methods allow us to create mice that express constitutively edited FLNB protein or lacking FLNB editing by deleting the ECS to test the exact effect of modified FLNB in these tissues. These mice are physically available already, but proper phenotypical and analytical studies of mice are missing to date. Also, ADAR expression correlating to editing levels and editing in ADAR knock-out mice must be examined to get an idea about the specificity of editing by ADAR1, ADAR2 or both.

Others had suggested regulation of Flnb editing in the circadian cycle (Terajima et al. 2017). To test this hypothesis, we prepared a library of twelve tissues isolated from one mouse in the morning and compared it with the editing of tissues taken in the afternoon. The editing events of this small library were compared with the average deamination in exon 42 of the library that was performed in triplicates. With our samples, we could not show and reproduce the data from the study mentioned above that showed that deamination events are higher in the morning hours.

To conclude, a lot of studies focus on the effect of editing and brain function and development, like GRIA2 and HTR2C (Kawahara et al. 2008). It has been proven that also filamins exhibit a specific function in the brain (Fox et al. 1998) and show editing levels of up to 38% in *Flna* mRNA. We could also show moderate levels of *Flnb* mRNA editing throughout the brain when

compared to *Flna* mRNA. The study previously performed by the Jantsch group demonstrated that the editing levels in brain tissues are by far not the highest and that there is a correlation between the organs where deletion of the respective filamin shows a phenotype and where editing is high. This correlation indicates a specific function of filamins in distinct organs other than the brain. To date, these specific functions of edited versus unedited versions of filamin b protein are poorly understood. Therefore, further studies have to be performed.

FLNA orthogonally crosslinks actin filaments and is responsible for the integrity and remodelling of the peripheral cytoskeleton, especially during cell motility. Due to its scaffolding function, FLNA is also involved in several cell-signalling pathways. Therefore, FLNA has been shown to play a role in cancer progression and metastasis (reviewed in Yue et al. 2013). In fact, it has been shown that reduction or deficiency of FLNA expression significantly reduces migration and invasion in cancer cells (Jiang et al. 2013). Similar studies discovered a general overexpression of FLNA in breast cancer compared to normal and benign breast tissues. High protein expression goes along with the elevated risk of metastasis and invasion, suggesting a contribution to cancer development and progression (Tian et al. 2013). We therefore analysed the contribution of edited and unedited FLNA protein on cancer cell proliferation.

Despite the modest expression of edited/unedited FLNA in stably transfected M2 cells as tested by immunofluorescence and by western blot (figure 14), we could detect differences in cell proliferation and colony formation. Concerning the growth curve, a proliferative advantage was shown in M2 cells expressing edited FLNA only after four days in culture, arguing for a positive effect of edited FLNA on proliferation. At the same time cell death could be a plausible cause for the decrease in cell count for M2 cells expressing unedited Flna. However, more foci are formed by unedited FLNA M2 clones when cells are seeded at low density. This assay tests the growth potential of a single cell in anchorage-permissive conditions. We also observe a loss of FLNA expression in this assay which may dampen the observed results. Therefore, a cell system guaranteeing a stable FLNA expression should be used in the future. Still, our data indicate that expression of unedited FLNA increases the potential to form colonies from single cells as we saw smaller but more colonies. The fact that colonies expressing unedited FLNA are small compared to those formed by cells expressing edited FLNA may result from the different growth rates seen in the proliferation assay. Different colony formation potential and different grow rates depending on the editing status of FLNA may also explain some of the antagonistic functions of FLNA in tumor formation (Savoy and Ghosh 2013).

To learn more about the interactome of edited and unedited FLNA we performed pulldown experiments. Excitingly we could identify conditions that allowed precipitation of FLNA from colon tissue. Future experiments will be required to study the interactome of FLNA using these conditions.

List of tables

List of figures

Deutsche Zusammenfassung

Modifikation von Nukleotiden in Ribonukleinsäuren (RNA) spielt eine wesentliche Rolle in Organismen und ist seit geraumer Zeit Bestandteil intensiver Forschungen. Eine dieser zahlreichen Modifikationen, die Editierung von Adenosin zu Inosin (A-zu-I), ist die am häufigsten in Erscheinung tretende RNA-Modifikation in Metazoen. Diese Veränderung wird sowohl während als auch nach der Transkription durchgeführt. Dabei sind Proteine der Familie der „Adenosindeaminases acting on RNAs“ (ADARs) für diese spezifische Modifikation verantwortlich. Die Grundvoraussetzung für die Modifikation eines Adenins ist die Formation eines Doppelstranges im RNA Molekül. ADAR Enzyme benötigen diese Struktur um mit ihren „double-stranded RNA-binding domains“ (dsRBD) daran binden zu können. Über die Deaminasedomäne der Enzyme findet in weiterer Folge eine hydrolytische Deaminierung und damit die Modifikation von Adenosin zu Inosin statt.

Die Deaminierung eines Adenosins am Kohlenstoffatom sechs der Nukleinsäure, führt zu einem Wechsel von einem Elektronendonor zu einem Elektronakzeptor. Dies führt dazu, dass diverse Zellmaschinerien das modifizierte Adenosin (=Inosin) als ein Guanosin interpretieren, da dieses Inosin ähnliche Wasserstoffbrückenbindungen eingeht. Dies kann Auswirkungen auf die Translation, die Reifung von micro-RNAs, das Spleißen von unreifer messenger RNA (mRNA) oder andere zelluläre Prozesse haben. In dieser Arbeit jedoch fokussieren wir uns ausschließlich auf die nicht synonyme Substitution von Aminosäuren als Folge der A-zu-I in der mRNA.

Das Gehirn ist das am meist studierte Organ bezüglich nicht synonymer Substitution von Aminosäuren durch ADARs. Der Glutamat-Rezeptor beispielsweise ist fast vollständig und permanent in einer seiner Untereinheiten editiert. Dies verhindert unkontrollierten Influx und damit die Aktivierung von Nervenzellen durch Kalzium Ionen durch die Modulation und Verminderung der Permeabilität dieser Untereinheit für diese Ionen. In Mäusen wurde gezeigt, dass das Fehlen dieser Modifikation Schlaganfälle auslöst und schlussendlich zum Tod im jungen Alter führt. Dieser Prozess der nicht synonymen Aminosäuresubstitution ist in Menschen hoch konserviert und ist bis heute bei ungefähr hundert Transkriptionsprodukten bekannt. Vergangene Studien, wie jene bezüglich des Glutamat-Rezeptors, haben gezeigt, dass dieser Prozess meist eine wichtige Funktion innehat.

In dieser Arbeit wollen wir uns weniger spezifisch auf das Gehirn, sondern auf den ganzen Körper konzentrieren. Hierbei fokussieren wir uns auf eine der wenigen mRNAs deren Aminosäuresequenz durch ADAR Modifikation verändert wird, nämlich Filamin B. Die beiden homologen Mitglieder der Familie der Filamine (A und B) werden jeweils an der gleichen Position editiert. Dies hat zur Folge, dass das Codon der RNA welches normal für ein Glutamat codiert, zu einem Codon für ein Arginin editiert wird.

Um ein Fundament für zukünftige Studien zu legen, war es unser Anliegen ein Profil der Editierungsrate des Transkriptionsproduktes des Filamin B Genes zu erstellen. Außerdem wollen wir den Fokus vom Hirn auf den gesamten Organismus legen, da wir der

Überzeugung sind, dass dieser Prozess auch in diversen anderen Geweben einen wesentlichen Einfluss auf zelluläre Prozesse haben kann. Daher wurden insgesamt vierundzwanzig verschiedene Organe der Maus in drei verschiedenen Entwicklungsstadien untersucht. Gewebe wurden von Mäusen direkt nach der Geburt, von Jungtieren (21 Tage nach der Geburt) und von adulten Mäuse (120 Tage nach der Geburt) entnommen. Folgend wurde RNA aus den Organen isoliert, komplementäre Desoxyribonukleinsäure durch reverse Transkription produziert und die spezifische Editierungssequenz mittels Polymerasen Kettenreaktion amplifiziert. Amplifikationsprodukte wurden durch neueste Sequenzierungsmethoden sequenziert und anschließend die Relation von editierter zu nicht editierter RNA pro Entwicklungsstadium und Organ analysiert.

Unsere Daten zeigen, dass Organe mit hoher Editierungsrate können zusammenfassend in den Bewegungsapparat eingeteilt werden. Darunter befinden sich flache als auch lange Knochen wie die der Schädelplatte und des Femur Knochens mit einer Modifikationsrate von bis zu 90%, sowie Knorpel und Muskel des Bewegungsapparates. Forschungsergebnisse haben gezeigt, dass Filamin B eine wesentliche Rolle in der Entwicklung der Knochen spielt, da der Verlust dieses Proteins zu Missbildungen und Verknöcherung in der Wirbelsäule, den Pfoten und der Mittelfußknöchel führt. Außerdem konnten wir erhöhte Editierungsraten in Fettgewebe, Herz und Blut feststellen.

Die Kenntnis, dass die Modifikation eines Proteins in bestimmten Organen erhöht ist, bestätigt die Annahme einer potenziell spezifischen Funktion die hinter dieser nicht synonymen Aminosäuren Substitution steckt. Wie dieser Wechsel von Glutamin zu Arginin die Funktion des Proteins und dessen Interaktion mit anderen Proteinen beeinflusst wird einer der nächsten Schritte sein.

Es wurde bereits berichtet, dass es in Tumorzellen zu einer Deregulation der Modifikation in Filaminen kommt. Um den Einfluss der Modifikation auf die Funktion des anderen Familienmitgliedes der Filamine (Filamin A) zu untersuchen, wurde daher ein Protokoll für die Proteinisolation von Filamin A entwickelt. Dieses Verfahren soll in Zukunft dazu dienen Filamin A für massenspektrometrische Methoden aus Zellen zu isolieren. Zusätzlich wurden Experimente durchgeführt welche Schlüsse über den Einfluss von editiertem und nicht editiertem Filamin A auf die Zellteilung und auf das Potenzial in Isolation Zellteilung zu betreiben zulassen sollen.

In unserem Proliferationstest konnten wir feststellen, dass Zellen welche ausschließlich editiertes Filamin A exprimieren, schnellere Zellteilung betreiben als jene Zellen ohne nicht synonymer Aminosäuren Substitution in diesem Protein. Die Ergebnisse des zweiten Experiments jedoch zeigen, dass Ziellinien mit nicht editiertem Filamin A ein erhöhtes Potential der Proliferation in Isolation innehaben. Unsere Daten sind vergleichbar mit bereits erschienen Studien welche zeigen, dass editiertes Filamin A sowohl pro- als auch anti-proliferativ wirken kann. Warum und wie diese Prozesse im Detail reguliert werden ist hoch interessant und wird Thema von zukünftigen Studien sein.

References

Bahn, J.H., Lee, J.-H., Li, G., Greer, C., Peng, G., and Xiao, X. (2012). Accurate identification of A-to-I RNA editing in human by transcriptome sequencing. Genome Res. *22*, 142–150.

Barry, C.P., Xie, J., Lemmon, V., and Young, A.P. (1993). Molecular characterization of a multi-promoter gene encoding a chicken filamin protein. J. Biol. Chem. *268*, 25577–25586.

Beghini, A., Ripamonti, C.B., Peterlongo, P., Roversi, G., Cairoli, R., Morra, E., and Larizza, L. (2000). RNA hyperediting and alternative splicing of hematopoietic cell phosphatase (PTPN6) gene in acute myeloid leukemia. Hum. Mol. Genet. *9*, 2297–2304.

Bellanger, J.M., Astier, C., Sardet, C., Ohta, Y., Stossel, T.P., and Debant, A. (2000). The Rac1- and RhoG-specific GEF domain of Trio targets filamin to remodel cytoskeletal actin. Nat. Cell Biol. *2*, 888–892.

Bhalla, T., Rosenthal, J.J.C., Holmgren, M., and Reenan, R. (2004). Control of human potassium channel inactivation by editing of a small mRNA hairpin. Nat. Struct. Mol. Biol. *11*, 950–956.

Bhansali, P., Dunning, J., Singer, S.E., David, L., and Schmauss, C. (2007). Early life stress alters adult serotonin 2C receptor pre-mRNA editing and expression of the alpha subunit of the heterotrimeric G-protein G q. J. Neurosci. *27*, 1467–1473.

Brotschi, E.A., Hartwig, J.H., and Stossel, T.P. (1978). The gelation of actin by actin-binding protein. J. Biol. Chem. *253*, 8988–8993.

Brusa, R., Zimmermann, F., Koh, D.S., Feldmeyer, D., Gass, P., Seeburg, P.H., and Sprengel, R. (1995). Early-onset epilepsy and postnatal lethality associated with an editing-deficient GluR-B allele in mice. Science *270*, 1677–1680.

Burns, C.M., Chu, H., Rueter, S.M., Hutchinson, L.K., Canton, H., Sanders-Bush, E., and Emeson, R.B. (1997). Regulation of serotonin-2C receptor G-protein coupling by RNA editing. Nature *387*, 303–308.

Cattaneo, R., Schmid, A., Eschle, D., Baczko, K., ter Meulen, V., and Billeter, M.A. (1988). Biased hypermutation and other genetic changes in defective measles viruses in human brain infections. Cell *55*, 255–265.

Chakarova, C., Wehnert, M.S., Uhl, K., Sakthivel, S., Vosberg, H.P., van der Ven, P.F., and Fürst, D.O. (2000). Genomic structure and fine mapping of the two human filamin gene paralogues FLNB and FLNC and comparative analysis of the filamin gene family. Hum. Genet. *107*, 597–611.

Chan, T.H.M., Lin, C.H., Qi, L., Fei, J., Li, Y., Yong, K.J., Liu, M., Song, Y., Chow, R.K.K., Ng, V.H.E., et al. (2014). A disrupted RNA editing balance mediated by ADARs (Adenosine DeAminases that act on RNA) in human hepatocellular carcinoma. Gut *63*, 832–843.

Chen, C.X., Cho, D.S., Wang, Q., Lai, F., Carter, K.C., and Nishikura, K. (2000). A third member of the RNA-specific adenosine deaminase gene family, ADAR3, contains both single- and double-stranded RNA binding domains. RNA *6*, 755–767.

Chen, H.S., Kolahi, K.S., and Mofrad, M.R.K. (2009). Phosphorylation facilitates the integrin binding of filamin under force. Biophys. J. *97*, 3095–3104.

Chilibeck, K.A., Wu, T., Liang, C., Schellenberg, M.J., Gesner, E.M., Lynch, J.M., and MacMillan, A.M. (2006). FRET analysis of in vivo dimerization by RNA-editing enzymes. J. Biol. Chem. *281*, 16530–16535.

Cho, D.-S.C., Yang, W., Lee, J.T., Shiekhattar, R., Murray, J.M., and Nishikura, K. (2003). Requirement of dimerization for RNA editing activity of adenosine deaminases acting on RNA. J. Biol. Chem. *278*, 17093–17102.

Danecek, P., Nellåker, C., McIntyre, R.E., Buendia-Buendia, J.E., Bumpstead, S., Ponting, C.P., Flint, J., Durbin, R., Keane, T.M., and Adams, D.J. (2012). High levels of RNA-editing site conservation amongst 15 laboratory mouse strains. Genome Biol. *13*, 26.

Daniel, C., Widmark, A., Rigardt, D., and Öhman, M. (2017). Editing inducer elements increases A-to-I editing efficiency in the mammalian transcriptome. Genome Biol. *18*, 195.

Dillman, A.A., Cookson, M.R., and Galter, D. (2016). ADAR2 affects mRNA coding sequence edits with only modest effects on gene expression or splicing in vivo. RNA Biol *13*, 15–24.

Eggington, J.M., Greene, T., and Bass, B.L. (2011). Predicting sites of ADAR editing in double-stranded RNA. Nat Commun *2*, 319.

Farajollahi, S., and Maas, S. (2010). Molecular diversity through RNA editing: a balancing act. Trends Genet. *26*, 221–230.

Feng, Y., and Walsh, C.A. (2004). The many faces of filamin: a versatile molecular scaffold for cell motility and signalling. Nat. Cell Biol. *6*, 1034–1038.

Feng, Y., Chen, M.H., Moskowitz, I.P., Mendonza, A.M., Vidali, L., Nakamura, F., Kwiatkowski, D.J., and Walsh, C.A. (2006). Filamin A (FLNA) is required for cell-cell contact in vascular development and cardiac morphogenesis. Proc. Natl. Acad. Sci. U.S.A. *103*, 19836–19841.

van der Flier, A., Kuikman, I., Kramer, D., Geerts, D., Kreft, M., Takafuta, T., Shapiro, S.S., and Sonnenberg, A. (2002). Different splice variants of filamin-B affect myogenesis, subcellular distribution, and determine binding to integrin [beta] subunits. J. Cell Biol. *156*, 361–376.

Fox, J.E. (1985). Identification of actin-binding protein as the protein linking the membrane skeleton to glycoproteins on platelet plasma membranes. J. Biol. Chem. *260*, 11970–11977.

Fox, J.W., Lamperti, E.D., Ekşioğlu, Y.Z., Hong, S.E., Feng, Y., Graham, D.A., Scheffer, I.E., Dobyns, W.B., Hirsch, B.A., Radtke, R.A., et al. (1998). Mutations in filamin 1 prevent migration of cerebral cortical neurons in human periventricular heterotopia. Neuron *21*, 1315–1325.

Fritz, J., Strehblow, A., Taschner, A., Schopoff, S., Pasierbek, P., and Jantsch, M.F. (2009). RNA-regulated interaction of transportin-1 and exportin-5 with the double-stranded RNA-binding domain regulates nucleocytoplasmic shuttling of ADAR1. Mol. Cell. Biol. *29*, 1487–1497.

Garncarz, W., Tariq, A., Handl, C., Pusch, O., and Jantsch, M.F. (2013). A high-throughput screen to identify enhancers of ADAR-mediated RNA-editing. RNA Biol *10*, 192–204.

George, C.X., and Samuel, C.E. (1999). Characterization of the 5'-flanking region of the human RNA-specific adenosine deaminase ADAR1 gene and identification of an interferon-inducible ADAR1 promoter. Gene *229*, 203–213.

George, C.X., Li, Z., Okonski, K.M., Toth, A.M., Wang, Y., and Samuel, C.E. (2009). Tipping the balance: antagonism of PKR kinase and ADAR1 deaminase functions by virus gene products. J. Interferon Cytokine Res. *29*, 477–487.

Gomer, R.H., and Lazarides, E. (1983). Switching of filamin polypeptides during myogenesis in vitro. J. Cell Biol. *96*, 321–329.

Gorlin, J.B., Yamin, R., Egan, S., Stewart, M., Stossel, T.P., Kwiatkowski, D.J., and Hartwig, J.H. (1990). Human endothelial actin-binding protein (ABP-280, nonmuscle filamin): a molecular leaf spring. J. Cell Biol. *111*, 1089–1105.

Gumireddy, K., Li, A., Kossenkov, A.V., Sakurai, M., Yan, J., Li, Y., Xu, H., Wang, J., Zhang, P.J., Zhang, L., et al. (2016). The mRNA-edited form of GABRA3 suppresses GABRA3-mediated Akt activation and breast cancer metastasis. Nat Commun *7*, 10715.

Gurevich, I., Tamir, H., Arango, V., Dwork, A.J., Mann, J.J., and Schmauss, C. (2002). Altered editing of serotonin 2C receptor pre-mRNA in the prefrontal cortex of depressed suicide victims. Neuron *34*, 349–356.

Han, S.-W., Kim, H.-P., Shin, J.-Y., Jeong, E.-G., Lee, W.-C., Kim, K.Y., Park, S.Y., Lee, D.-W., Won, J.-K., Jeong, S.-Y., et al. (2014). RNA editing in RHOQ promotes invasion potential in colorectal cancer. J. Exp. Med. *211*, 613–621.

Hart, A.W., Morgan, J.E., Schneider, J., West, K., McKie, L., Bhattacharya, S., Jackson, I.J., and Cross, S.H. (2006). Cardiac malformations and midline skeletal defects in mice lacking filamin A. Hum. Mol. Genet. *15*, 2457–2467.

Hartner, J.C., Walkley, C.R., Lu, J., and Orkin, S.H. (2009). ADAR1 is essential for the maintenance of hematopoiesis and suppression of interferon signaling. Nat. Immunol. *10*, 109–115.

Higuchi, M., Single, F.N., Köhler, M., Sommer, B., Sprengel, R., and Seeburg, P.H. (1993). RNA editing of AMPA receptor subunit GluR-B: a base-paired intron-exon structure determines position and efficiency. Cell *75*, 1361–1370.

Higuchi, M., Maas, S., Single, F.N., Hartner, J., Rozov, A., Burnashev, N., Feldmeyer, D., Sprengel, R., and Seeburg, P.H. (2000). Point mutation in an AMPA receptor gene rescues lethality in mice deficient in the RNA-editing enzyme ADAR2. Nature *406*, 78–81.

Hung, L.-Y., Chen, Y.-J., Mai, T.-L., Chen, C.-Y., Yang, M.-Y., Chiang, T.-W., Wang, Y.-D., and Chuang, T.-J. (2018). An Evolutionary Landscape of A-to-I RNA Editome across Metazoan Species. Genome Biol Evol *10*, 521–537.

Hwang, T., Park, C.-K., Leung, A.K.L., Gao, Y., Hyde, T.M., Kleinman, J.E., Rajpurohit, A., Tao, R., Shin, J.H., and Weinberger, D.R. (2016). Dynamic regulation of RNA editing in human brain development and disease. Nat. Neurosci. *19*, 1093–1099.

Iizasa, H., Wulff, B.-E., Alla, N.R., Maragkakis, M., Megraw, M., Hatzigeorgiou, A., Iwakiri, D., Takada, K., Wiedmer, A., Showe, L., et al. (2010). Editing of Epstein-Barr virus-encoded BART6 microRNAs controls their dicer targeting and consequently affects viral latency. J. Biol. Chem. *285*, 33358–33370.

Jain, M., Mann, T.D., Stulić, M., Rao, S.P., Kirsch, A., Pullirsch, D., Strobl, X., Rath, C., Reissig, L., Moreth, K., et al. (2018). RNA editing of Filamin A pre-mRNA regulates vascular contraction and diastolic blood pressure. EMBO J.

Janmey, P.A., Hvidt, S., Lamb, J., and Stossel, T.P. (1990). Resemblance of actin-binding protein/actin gels to covalently crosslinked networks. Nature *345*, 89–92.

Jay, D., García, E.J., Lara, J.E., Medina, M.A., and de la Luz Ibarra, M. (2000). Determination of a cAMP-dependent protein kinase phosphorylation site in the C-terminal region of human endothelial actin-binding protein. Arch. Biochem. Biophys. *377*, 80–84.

Jiang, X., Yue, J., Lu, H., Campbell, N., Yang, Q., Lan, S., Haffty, B.G., Yuan, C., and Shen, Z. (2013). Inhibition of filamin-A reduces cancer metastatic potential. Int. J. Biol. Sci. *9*, 67–77.

Kawahara, Y., Zinshteyn, B., Chendrimada, T.P., Shiekhattar, R., and Nishikura, K. (2007). RNA editing of the microRNA-151 precursor blocks cleavage by the Dicer-TRBP complex. EMBO Rep. *8*, 763–769.

Kawahara, Y., Grimberg, A., Teegarden, S., Mombereau, C., Liu, S., Bale, T.L., Blendy, J.A., and Nishikura, K. (2008). Dysregulated editing of serotonin 2C receptor mRNAs results in energy dissipation and loss of fat mass. J. Neurosci. *28*, 12834–12844.

Krampfl, K., Schlesinger, F., Zörner, A., Kappler, M., Dengler, R., and Bufler, J. (2002). Control of kinetic properties of GluR2 flop AMPA-type channels: impact of R/G nuclear editing. Eur. J. Neurosci. *15*, 51–62.

Lehmann, K.A., and Bass, B.L. (1999). The importance of internal loops within RNA substrates of ADAR1. J. Mol. Biol. *291*, 1–13.

Lei, M., Liu, Y., and Samuel, C.E. (1998). Adenovirus VAI RNA antagonizes the RNA-editing activity of the ADAR adenosine deaminase. Virology *245*, 188–196.

Lei, T., Yuen, K.-S., Tsao, S.W., Chen, H., Kok, K.-H., and Jin, D.-Y. (2013). Perturbation of biogenesis and targeting of Epstein-Barr virus-encoded miR-BART3 microRNA by adenosine-to-inosine editing. J. Gen. Virol. *94*, 2739–2744.

Leonardi, A., Ellinger-Ziegelbauer, H., Franzoso, G., Brown, K., and Siebenlist, U. (2000). Physical and functional interaction of filamin (actin-binding protein-280) and tumor necrosis factor receptor-associated factor 2. J. Biol. Chem. *275*, 271–278.

Lev-Maor, G., Ram, O., Kim, E., Sela, N., Goren, A., Levanon, E.Y., and Ast, G. (2008). Intronic Alus influence alternative splicing. PLoS Genet. *4*, e1000204.

Li, J.B., Levanon, E.Y., Yoon, J.-K., Aach, J., Xie, B., Leproust, E., Zhang, K., Gao, Y., and Church, G.M. (2009). Genome-wide identification of human RNA editing sites by parallel DNA capturing and sequencing. Science *324*, 1210–1213.

Lomeli, H., Mosbacher, J., Melcher, T., Höger, T., Geiger, J.R., Kuner, T., Monyer, H., Higuchi, M., Bach, A., and Seeburg, P.H. (1994). Control of kinetic properties of AMPA receptor channels by nuclear RNA editing. Science *266*, 1709–1713.

Maas, S., and Gommans, W.M. (2009). Identification of a selective nuclear import signal in adenosine deaminases acting on RNA. Nucleic Acids Res. *37*, 5822–5829.

Maas, S., Patt, S., Schrey, M., and Rich, A. (2001). Underediting of glutamate receptor GluR-B mRNA in malignant gliomas. Proc. Natl. Acad. Sci. U.S.A. *98*, 14687–14692.

Macbeth, M.R., Schubert, H.L., Vandemark, A.P., Lingam, A.T., Hill, C.P., and Bass, B.L. (2005). Inositol hexakisphosphate is bound in the ADAR2 core and required for RNA editing. Science *309*, 1534–1539.

Mannion, N.M., Greenwood, S.M., Young, R., Cox, S., Brindle, J., Read, D., Nellåker, C., Vesely, C., Ponting, C.P., McLaughlin, P.J., et al. (2014). The RNA-editing enzyme ADAR1 controls innate immune responses to RNA. Cell Rep *9*, 1482–1494.

Meyer, S.C., Sanan, D.A., and Fox, J.E. (1998). Role of actin-binding protein in insertion of adhesion receptors into the membrane. J. Biol. Chem. *273*, 3013–3020.

Miyamura, Y., Suzuki, T., Kono, M., Inagaki, K., Ito, S., Suzuki, N., and Tomita, Y. (2003). Mutations of the RNA-specific adenosine deaminase gene (DSRAD) are involved in dyschromatosis symmetrica hereditaria. Am. J. Hum. Genet. *73*, 693–699.

Nakamura, F., Stossel, T.P., and Hartwig, J.H. (2011). The filamins: organizers of cell structure and function. Cell Adh Migr *5*, 160–169.

Nigita, G., Veneziano, D., and Ferro, A. (2015). A-to-I RNA Editing: Current Knowledge Sources and Computational Approaches with Special Emphasis on Non-Coding RNA Molecules. Front Bioeng Biotechnol *3*, 37.

Nishikura, K. (2010). Functions and Regulation of RNA Editing by ADAR Deaminases. Annu Rev Biochem *79*, 321–349.

Nishikura, K. (2016). A-to-I editing of coding and non-coding RNAs by ADARs. Nat. Rev. Mol. Cell Biol. *17*, 83–96.

Nishikura, K., Yoo, C., Kim, U., Murray, J.M., Estes, P.A., Cash, F.E., and Liebhaber, S.A. (1991). Substrate specificity of the dsRNA unwinding/modifying activity. EMBO J. *10*, 3523–3532.

Ohta, Y., Suzuki, N., Nakamura, S., Hartwig, J.H., and Stossel, T.P. (1999). The small GTPase RalA targets filamin to induce filopodia. Proc. Natl. Acad. Sci. U.S.A. *96*, 2122–2128.

Ota, H., Sakurai, M., Gupta, R., Valente, L., Wulff, B.-E., Ariyoshi, K., Iizasa, H., Davuluri, R.V., and Nishikura, K. (2013). ADAR1 forms a complex with Dicer to promote microRNA processing and RNA-induced gene silencing. Cell *153*, 575–589.

Patrosso, M.C., Repetto, M., Villa, A., Milanesi, L., Frattini, A., Faranda, S., Mancini, M., Maestrini, E., Toniolo, D., and Vezzoni, P. (1994). The exon-intron organization of the human X-linked gene (FLN1) encoding actin-binding protein 280. Genomics *21*, 71–76.

Patterson, J.B., and Samuel, C.E. (1995). Expression and regulation by interferon of a double-stranded-RNA-specific adenosine deaminase from human cells: evidence for two forms of the deaminase. Mol Cell Biol *15*, 5376–5388.

Paz, N., Levanon, E.Y., Amariglio, N., Heimberger, A.B., Ram, Z., Constantini, S., Barbash, Z.S., Adamsky, K., Safran, M., Hirschberg, A., et al. (2007). Altered adenosine-to-inosine RNA editing in human cancer. Genome Res. *17*, 1586–1595.

Peng, P.L., Zhong, X., Tu, W., Soundarapandian, M.M., Molner, P., Zhu, D., Lau, L., Liu, S., Liu, F., and Lu, Y. (2006). ADAR2-dependent RNA editing of AMPA receptor subunit GluR2 determines vulnerability of neurons in forebrain ischemia. Neuron *49*, 719–733.

Pfaff, M., Liu, S., Erle, D.J., and Ginsberg, M.H. (1998). Integrin beta cytoplasmic domains differentially bind to cytoskeletal proteins. J. Biol. Chem. *273*, 6104–6109.

Popowicz, G.M., Schleicher, M., Noegel, A.A., and Holak, T.A. (2006). Filamins: promiscuous organizers of the cytoskeleton. Trends Biochem. Sci. *31*, 411–419.

Pudas, R., Kiema, T.-R., Butler, P.J.G., Stewart, M., and Ylänne, J. (2005). Structural basis for vertebrate filamin dimerization. Structure *13*, 111–119.

Qin, Y.-R., Qiao, J.-J., Chan, T.H.M., Zhu, Y.-H., Li, F.-F., Liu, H., Fei, J., Li, Y., Guan, X.-Y., and Chen, L. (2014). Adenosine-to-inosine RNA editing mediated by ADARs in esophageal squamous cell carcinoma. Cancer Res. *74*, 840–851.

Ramaswami, G., Zhang, R., Piskol, R., Keegan, L.P., Deng, P., O'Connell, M.A., and Li, J.B. (2013). Identifying RNA editing sites using RNA sequencing data alone. Nat. Methods *10*, 128–132.

Rueter, S.M., Dawson, T.R., and Emeson, R.B. (1999). Regulation of alternative splicing by RNA editing. Nature *399*, 75–80.

Savoy, R.M., and Ghosh, P.M. (2013). The dual role of filamin A in cancer: can't live with (too much of) it, can't live without it. Endocr. Relat. Cancer *20*, R341-356.

Sheen, V.L., Feng, Y., Graham, D., Takafuta, T., Shapiro, S.S., and Walsh, C.A. (2002). Filamin A and Filamin B are co-expressed within neurons during periods of neuronal migration and can physically interact. Hum. Mol. Genet. *11*, 2845–2854.

Shimokawa, T., Rahman, M.F.-U., Tostar, U., Sonkoly, E., Ståhle, M., Pivarcsi, A., Palaniswamy, R., and Zaphiropoulos, P.G. (2013). RNA editing of the GLI1 transcription factor modulates the output of Hedgehog signaling. RNA Biol *10*, 321–333.

Sommer, B., Köhler, M., Sprengel, R., and Seeburg, P.H. (1991). RNA editing in brain controls a determinant of ion flow in glutamate-gated channels. Cell *67*, 11–19.

Stellos, K., Gatsiou, A., Stamatelopoulos, K., Perisic Matic, L., John, D., Lunella, F.F., Jaé, N., Rossbach, O., Amrhein, C., Sigala, F., et al. (2016). Adenosine-to-inosine RNA editing controls cathepsin S expression in atherosclerosis by enabling HuR-mediated post-transcriptional regulation. Nat. Med. *22*, 1140–1150.

Stossel, T.P., Condeelis, J., Cooley, L., Hartwig, J.H., Noegel, A., Schleicher, M., and Shapiro, S.S. (2001). Filamins as integrators of cell mechanics and signalling. Nat. Rev. Mol. Cell Biol. *2*, 138–145.

Stulić, M., and Jantsch, M.F. (2013). Spatio-temporal profiling of Filamin A RNA-editing reveals ADAR preferences and high editing levels outside neuronal tissues. RNA Biol *10*, 1611–1617.

Tajaddod, M., Tanzer, A., Licht, K., Wolfinger, M.T., Badelt, S., Huber, F., Pusch, O., Schopoff, S., Janisiw, M., Hofacker, I., et al. (2016). Transcriptome-wide effects of inverted SINEs on gene expression and their impact on RNA polymerase II activity. Genome Biol. *17*, 220.

Takafuta, T., Wu, G., Murphy, G.F., and Shapiro, S.S. (1998). Human beta-filamin is a new protein that interacts with the cytoplasmic tail of glycoprotein Ibalpha. J. Biol. Chem. *273*, 17531–17538.

Tan, M.H., Li, Q., Shanmugam, R., Piskol, R., Kohler, J., Young, A.N., Liu, K.I., Zhang, R., Ramaswami, G., Ariyoshi, K., et al. (2017). Dynamic landscape and regulation of RNA editing in mammals. Nature *550*, 249–254.

Terajima, H., Yoshitane, H., Ozaki, H., Suzuki, Y., Shimba, S., Kuroda, S., Iwasaki, W., and Fukada, Y. (2017). ADARB1 catalyzes circadian A-to-I editing and regulates RNA rhythm. Nat. Genet. *49*, 146–151.

Thompson, T.G., Chan, Y.M., Hack, A.A., Brosius, M., Rajala, M., Lidov, H.G., McNally, E.M., Watkins, S., and Kunkel, L.M. (2000). Filamin 2 (FLN2): A muscle-specific sarcoglycan interacting protein. J. Cell Biol. *148*, 115–126.

Tian, H.-M., Liu, X.-H., Han, W., Zhao, L.-L., Yuan, B., and Yuan, C.-J. (2013). Differential expression of filamin A and its clinical significance in breast cancer. Oncol Lett *6*, 681–686.

Tojo, K., Sekijima, Y., Suzuki, T., Suzuki, N., Tomita, Y., Yoshida, K., Hashimoto, T., and Ikeda, S.-I. (2006). Dystonia, mental deterioration, and dyschromatosis symmetrica hereditaria in a family with ADAR1 mutation. Mov. Disord. *21*, 1510–1513.

Ueda, M., Oho, C., Takisawa, H., and Ogihara, S. (1992). Interaction of the low-molecular-mass, guanine-nucleotide-binding protein with the actin-binding protein and its modulation by the cAMP-dependent protein kinase in bovine platelets. Eur. J. Biochem. *203*, 347–352.

Valente, L., and Nishikura, K. (2007). RNA binding-independent dimerization of adenosine deaminases acting on RNA and dominant negative effects of nonfunctional subunits on dimer functions. J. Biol. Chem. *282*, 16054–16061.

Vesely, C., Tauber, S., Sedlazeck, F.J., von Haeseler, A., and Jantsch, M.F. (2012). Adenosine deaminases that act on RNA induce reproducible changes in abundance and sequence of embryonic miRNAs. Genome Res. *22*, 1468–1476.

Wang, Q., Miyakoda, M., Yang, W., Khillan, J., Stachura, D.L., Weiss, M.J., and Nishikura, K. (2004). Stress-induced apoptosis associated with null mutation of ADAR1 RNA editing deaminase gene. J. Biol. Chem. *279*, 4952–4961.

Wong, S.K., Sato, S., and Lazinski, D.W. (2001). Substrate recognition by ADAR1 and ADAR2. RNA *7*, 846–858.

Wu, D., Lamm, A.T., and Fire, A.Z. (2011). Competition between ADAR and RNAi pathways for an extensive class of RNA targets. Nat. Struct. Mol. Biol. *18*, 1094–1101.

XuFeng, R., Boyer, M.J., Shen, H., Li, Y., Yu, H., Gao, Y., Yang, Q., Wang, Q., and Cheng, T. (2009). ADAR1 is required for hematopoietic progenitor cell survival via RNA editing. Proc. Natl. Acad. Sci. U.S.A. *106*, 17763–17768.

Yada, Y., Okano, Y., and Nozawa, Y. (1990). Enhancement of GTP gamma S-binding activity by cAMP-dependent phosphorylation of a filamin-like 250 kDa membrane protein in human platelets. Biochem. Biophys. Res. Commun. *172*, 256–261.

Yang, L., Huang, P., Li, F., Zhao, L., Zhang, Y., Li, S., Gan, Z., Lin, A., Li, W., and Liu, Y. (2012). c-Jun amino-terminal kinase-1 mediates glucose-responsive upregulation of the RNA editing enzyme ADAR2 in pancreatic beta-cells. PLoS ONE *7*, e48611.

Yeo, J., Goodman, R.A., Schirle, N.T., David, S.S., and Beal, P.A. (2010). RNA editing changes the lesion specificity for the DNA repair enzyme NEIL1. Proc. Natl. Acad. Sci. U.S.A. *107*, 20715–20719.

Yue, J., Huhn, S., and Shen, Z. (2013). Complex roles of filamin-A mediated cytoskeleton network in cancer progression. Cell Biosci *3*, 7.

Zhou, A.-X., Hartwig, J.H., and Akyürek, L.M. (2010). Filamins in cell signaling, transcription and organ development. Trends Cell Biol. *20*, 113–123.

Zhou, X., Tian, F., Sandzén, J., Cao, R., Flaberg, E., Szekely, L., Cao, Y., Ohlsson, C., Bergo, M.O., Borén, J., et al. (2007). Filamin B deficiency in mice results in skeletal malformations and impaired microvascular development. Proc. Natl. Acad. Sci. U.S.A. *104*, 3919–3924.

Zieba, J., Forlenza, K.N., Khatra, J.S., Sarukhanov, A., Duran, I., Rigueur, D., Lyons, K.M., Cohn, D.H., Merrill, A.E., and Krakow, D. (2016). TGFβ and BMP Dependent Cell Fate Changes Due to Loss of Filamin B Produces Disc Degeneration and Progressive Vertebral Fusions. PLoS Genet. *12*, e1005936.